J. Fluid Mech. (1984), *vol.* 141, *pp.* 319–345
Printed in Great Britain

Non-uniqueness and stability of the configuration of flow of immiscible fluids with different viscosities

By D. D. JOSEPH, K. NGUYEN AND G. S. BEAVERS
University of Minnesota, Minneapolis 55455

(Received 19 April 1983 and in revised form 20 October 1983)

High-viscosity liquids hate to work. Low-viscosity liquids are the victims of the laziness of high-viscosity liquids because they are easy to push around.

The arrangement of components in steady flow of immiscible liquids is typically non-unique. The problem of selection of arrangements is defined here and is studied by variational methods under the hypothesis that the realized arrangements are the ones that maximize the speed on exterior boundaries for prescribed boundary tractions, or the ones that minimize the tractions for prescribed speeds. The arrangements which minimize tractions also minimize the dissipation by putting low-viscosity liquid in regions of high shear. The variational problem is used as a guide to intuition in the design and interpretation of experiments when results of analysis of stability are unavailable. In fact we always observe some kind of shielding of high-viscosity liquid. This can occur by sheet coating in which low-viscosity liquid encapsulates high-viscosity liquid, or through the formation of rigidly rotating masses of high-viscosity liquid which we call rollers. In other cases we get emulsions of low-viscosity liquid in a high-viscosity foam. The emulsions arise from a fingering instability. The low-viscosity liquid fingers into the high-viscosity liquid and then low-viscosity bubbles are pinched off the fingers. The emulsions seem to have a very low effective viscosity and they shield the high-viscosity liquid from shearing. In the problem of Taylor instability with two fluids, low-viscosity Taylor cells are separated by stable high-viscosity rollers.

1. Introduction

We are interested in the flow of two immiscible liquids separated by an interface, driven by prescribed forces of the usual type. We call such motions bicomponent or two-phase flows. In fact, we do not consider two phases of the same material, but of separate liquids which do not mix (oil and water, for example). To fix our problem, we specify the total volume of the two fluids and the individual volumes occupied by each one of them. Then our problem is to describe the motion and the spatial arrangement of each component. There is a high degree of non-uniqueness in such problems, even when the motion is steady and even when the region of flow is bounded and the Reynolds numbers for each of the fluids is very small. In some cases we may find a class of steady motions: no motions, Couette motions, Poiseuille motions, etc. which are uniquely determined by the data up to an arbitrary rearrangement of components (phases). The arrangement of components that is actually achieved in the flow is certainly connected to the problem of hydrodynamic stability. However, it has been suggested that in some problems the configurations that are selected are

those which in some sense extremize the viscous dissipation. In fact a more precise statement of this criterion for selection can be formalized in terms of fluxes and forces. The idea is to maximize the flux for a given force (or to minimize the force for a given flux) over an admissible class of phase arrangements in a set of non-unique steady solutions. Our experiments show that something like this is going on. The arrangements of the components do in fact appear to be ones which extremize in some mathematical sense. The extremizing configurations are such as to minimize the shearing of high-viscosity liquids by the spontaneous migration of low-viscosity liquids into regions where the shearing is greatest. We shall call this tendency for low-viscosity liquids to migrate into the regions of high shears an *encapsulation* instability. A *fingering* instability that is responsible for the formation of emulsions is also important in the context of encapsulation. These types of instability are important because they represent a type of self-lubrication principle.

Ultimately the only satisfactory theoretical approach to the problem of selection is through stability. It is probable that most of the possible steady configurations of flow are unstable. The problem of stability of immiscible liquids with different viscosities has been considered by Yih (1967), Hooper & Boyd (1983) and Joseph, Renardy & Renardy (1984). In the latter paper, which we shall identify by JRR (1984), the problem of stability is clearly identified as a problem of selection of stable arrangement of components.

The preferred arrangements of components in bicomponent flow may be sought through variational principles associated with extremizing the dissipation. Although variational ideas are ambiguous in this problem of selection, we found that they provided useful guides in the design of our experiments.

The experiments reported in this paper seem to be of extraordinary interest in that they exhibit previously unknown types of fluid dynamics which may be typical for flows of immiscible liquids. Our experiments are visual and qualitative. In the future it would be good to monitor torques and speeds systematically and to undertake to correlate observations with systematic variations of geometric parameters.

2. Equations of motion

The equations of motion in each liquid are the usual ones. In our discussions of variational principles and for most of the experiments we report in this paper we shall consider Navier–Stokes fluids, but we are not yet certain that Navier–Stokes dynamics suffices to explain all that we have observed. The stress $\boldsymbol{T}$ is given by

$$\boldsymbol{T} = -p\boldsymbol{I} + \boldsymbol{S}, \quad \boldsymbol{S} = 2\mu \boldsymbol{D}[\boldsymbol{u}]. \tag{2.1}$$

Here $\boldsymbol{D}$ is $\frac{1}{2}$ of the symmetric part of the velocity gradient $\nabla \boldsymbol{u}$, and for all fluids in all regions of flow

$$\operatorname{div} \boldsymbol{u}_l = 0 \quad (l = 1, 2), \tag{2.2}$$

$$\rho \frac{\mathrm{d}}{\mathrm{d}t} \boldsymbol{u}_l = -\nabla \Phi_l + \operatorname{div} \boldsymbol{S}_l, \quad \boldsymbol{S}_l = 2\mu_l \boldsymbol{D}[\boldsymbol{u}_l], \tag{2.3}$$

$$\Phi_l = \rho_l g Z + p_l, \tag{2.4}$$

where g is gravity, Z increases against $\boldsymbol{g}$, ρ_1 and ρ_2 are the densities of the first and second fluids and μ_1 and μ_2 are the viscosities.

The interface between the regions 1 and 2 is called Σ and is given by

$$f(\boldsymbol{x}(t), t) = 0 \tag{2.5}$$

and, since this is an identity in t,

$$\frac{\partial f}{\partial t}+\boldsymbol{u}\cdot\nabla f=0, \tag{2.6}$$

where we have assumed that the normal component of velocity $\mathrm{d}\boldsymbol{x}/\mathrm{d}t$ of the surface Σ and the particles of fluid on either side of Σ are the same. In fact, the velocity $\boldsymbol{u}$ is continuous across Σ:

$$[\![\boldsymbol{u}]\!]=\boldsymbol{u}_1-\boldsymbol{u}_2=0. \tag{2.7}$$

Now we state the conditions of continuity for the stresses across Σ. Let $\boldsymbol{n}=\nabla f/|\nabla f|$ be the normal to Σ and let $\boldsymbol{\tau}_1$, $\boldsymbol{\tau}_2$ be two orthonormal vectors in Σ. The jump across Σ of the traction $[\boldsymbol{T}]\cdot\boldsymbol{n}$ satisfies

$$[\![\boldsymbol{T}]\!]\cdot\boldsymbol{n}+\nabla_{\mathrm{II}}\sigma+2H\sigma\boldsymbol{n}=0, \tag{2.8}$$

where ∇_{II} is a surface gradient, $2H$ is the sum of the principal curvatures and σ is surface tension. Now, using (2.4) we introduce the head Φ,

$$[\![\boldsymbol{T}]\!]=-[\![p]\!]\boldsymbol{I}+[\![\boldsymbol{S}]\!]=-[\![\Phi]\!]\boldsymbol{I}+g[\![\rho]\!]Z_\Sigma\boldsymbol{I}+[\![\boldsymbol{S}]\!], \tag{2.9}$$

where Z_Σ is the value of the coordinate Z on Σ. We project (2.8) using (2.9), with $\boldsymbol{n}$ and $\boldsymbol{\tau}_1, \boldsymbol{\tau}_2$ to find that

$$-[\![\Phi]\!]+\boldsymbol{n}\cdot[\![\boldsymbol{S}]\!]\cdot\boldsymbol{n}+gZ_\Sigma[\![\rho]\!]+2H\sigma=0, \tag{2.10}$$

$$\boldsymbol{\tau}_l\cdot[\![\boldsymbol{S}]\!]\cdot\boldsymbol{n}+\boldsymbol{\tau}_l\cdot\nabla_{\mathrm{II}}\sigma=0 \quad (l=1,2). \tag{2.11}$$

This statement of conditions is completed by stating boundary and other auxiliary conditions. In general the position of the interface, $f(x,t)=0$, is an unknown quantity, to be determined. In many cases, even after specifying the volumes occupied by each fluid, the solutions of the equations are not uniquely determined by the boundary data. In fact, there is a very high degree of non-uniqueness, which we shall now specify more precisely.

3. Examples of non-uniqueness in the steady flow of immiscible liquids

In this section we draw attention to some elementary configurations of two immiscible liquids which are not unique.

It is well known that immiscible liquids of the same density will form spheres of one liquid in another. The steady distribution of such spheres, their sizes and their placement seems not to be unique. In fact Plateau (1873) suspended masses of olive oil in a mixture of alcohol (lighter than oil) and water (heavier than oil) of the same density. By the latter device spheres of many centimetres were obtained. It is possible to have big spheres of oil in alcohol–water and big spheres of alcohol–water in oil. For such spheres we satisfy the equations of §2 with

$$\boldsymbol{u}=\boldsymbol{S}=\nabla_{\mathrm{II}}\sigma=[\![\rho]\!]=0 \quad \text{and} \quad 2H\sigma=[\![\Phi]\!]=[\![p]\!]=\frac{2\sigma}{R},$$

where R is the radius of each sphere. There is nothing here to determine the size and placement of spheres from given data.

The type of stationary configuration with bubbles of different sizes in immiscible fluids of matched density which was studied by Plateau is shown in figure 1 (plate 1). This figure shows the result of matching the density ($\rho=1.04$ g/cm^3) of dibutyl phthalate with a glycerol (heavier, $\rho=1.25$ g/cm^3) and water (lighter, $\rho=1.00$ g/cm^3) solution.

The non-unique stationary configurations that are achieved by matching density appear to be stable to small disturbances. However, there is a tendency for bubbles that touch to collapse into one bubble. It may be true that there is a selection mechanism based on stability to large disturbances in which the stable configuration is the one which minimizes surface area. This type of criterion leads to large bubbles, even one large one, rather than many small ones.

The number and size of successive layers of two liquids in layered plane Couette or plane Poiseuille flows are not uniquely determined by the Navier–Stokes equations and the appropriate interface and boundary conditions for steady motions. The same type of lack of uniqueness holds for Couette flow in circles and for the rectilinear motions of two liquids down pipes. Experiments with Poiseuille flows down pipes suggest that there is a tendency for the low-viscosity liquid to encapsulate the high-viscosity liquid. Two further examples of non-uniqueness of the configuration of components in bicomponent flow are the problem of one fluid displacing another in a pipe and convection in a fluid layer heated from below with two immiscible components of the same average density (Busse 1982).

In our experiments we see many different configurations. There are persistent solutions with bubbles of low-viscosity fluid in high-viscosity foams, which are steady in some average sense. We conclude that, unlike single-component flow, there is a pervasive lack of uniqueness in the flow of immiscible liquids even when the Reynolds number is small and even when the region of flow is bounded.

4. Extremal principles and variational problems

4.1. *Encapsulation instabilities and extremal principles for pipe flow*

In pipe flow of two liquids with different viscosities under an applied pressure drop, the low-viscosity liquid will tend to encapsulate the high-viscosity liquid. If the effects of gravity are negligible, the phases will arrange themselves so whatever may have been the initial configuration, the high-viscosity phase will ultimately be centrally located. This property has been convincingly demonstrated in experiments with very viscous viscoelastic liquids (polymer melts) by Southern & Ballman (1973), Everage (1973), Lee & White (1974), Williams (1975) and Minagawa & White (1975), as well as in the flow of oil and water, in which the water migrates to the pipe wall, forming a lubrication layer, studied by Charles & Redberger (1962), Hasson, Mann & Nir (1970) and Yu & Sparrow (1967).

In the experiments of Southern & Ballman (1973) encapsulation of the type exhibited in figure 2 is documented. Everage (1973) shows a photograph of complete encapsulation with a centrally located high-viscosity nylon completely encapsulated by an annular ring of low-viscosity fluid.

Theoretical explanations of the slow envelopment phenomenon have up to now been based upon extremizing energy dissipation as originally suggested by Southern & Ballman (1973). Maclean (1973), who considered planar layered flow, and Everage (1973), who studied a cylindrical geometry, both invoked a variational principle to show that the phase configuration with the high-viscosity component centrally located is favoured over several other configurations.

We are going to state a general variational criterion which presumably reduces to the ones first discussed for special cases. We say that realized flows arrange the two components so as to maximize the speeds when the tractions on exterior boundaries are fixed, or to minimize the tractions when the speeds are prescribed. For pipe flow we arrange the two flowing components to maximize the mass flux when the pressure

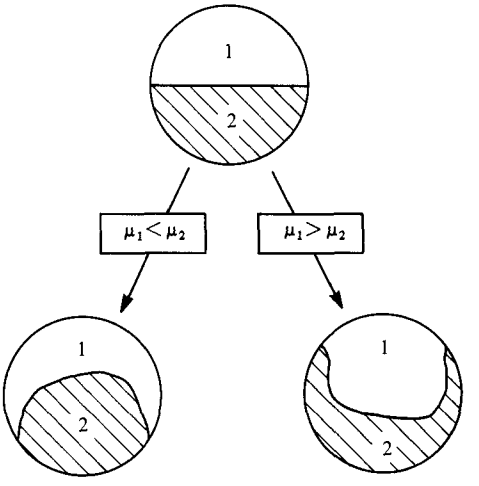

FIGURE 2. Encapsulation of high-viscosity liquid by low-viscosity liquid in pipe flow of polymer melts (after Southern & Ballman 1973).

gradient is prescribed or to minimize the pressure gradient when the mass flux is prescribed. The extremizing arrangement is the one with high-viscosity liquid in the centre (JRR 1984). We could draw an analogy with turbulent flow in which it is shown that, among all the turbulent solutions, the laminar one maximizes the mass flux for a given pressure drop. In fact the extremizing solution is not always stable. The results (JRR 1984) depend on the volume ratio with stable flows characterized by narrow layers of less viscous fluid on the outside.

The variational criterion just stated is not the only one possible. Instead of maximizing the total flux we might try to maximize the flux of one component (for example oil, viscosity μ_1) alone in a round pipe of radius R by lubricating the pipe wall with a liquid of lower viscosity μ_2, for example water. We suppose that the water fully encapsulates the oil in a central core of radius a. We shall find the a that maximizes the flow rate. The configuration determined by this a is in fact stable according to the calculations given in JRR (1984).

The velocity distributions in the two liquids are

$$u_1 = \frac{R^2}{4\mu_1} G \frac{a^2}{R^2} \left\{ \frac{\mu_1}{\mu_2} \left(\frac{R^2}{a^2} - 1 \right) + 1 - \frac{r^2}{a^2} \right\} \quad (0 \leqslant r \leqslant a)$$

and

$$u_2 = \frac{R^2}{4\mu_1} G \frac{a^2}{R^2} \frac{\mu_1}{\mu_2} \left(\frac{R^2}{a^2} - \frac{r^2}{a^2} \right) \quad (a \leqslant r \leqslant R),$$

where $G \equiv -\mathrm{d}p/\mathrm{d}x$. The volume flow rate of oil (Q_1) is then

$$\frac{Q_1}{\tilde{Q}} = \frac{a^4}{R^4} \left\{ 1 + 2 \frac{\mu_1}{\mu_2} \left(\frac{R^2}{a^2} - 1 \right) \right\},$$

where $\tilde{Q} = (R^4/8\mu_1) G$ is the volume flow rate of the single phase (μ_1) when it fills the entire pipe. For fixed R and G, the volume flow rate Q_1 has a maximum when

$$\frac{a}{R} = \left[\frac{\mu_1/\mu_2}{2\mu_1/\mu_2 - 1} \right]^{\frac{1}{2}},$$

and the maximum value is then

$$\left.\frac{Q_1}{\bar{Q}}\right|_{\max} = \frac{(\mu_1/\mu_2)^2}{2(\mu_1/\mu_2)-1}.$$

For large values of the viscosity ratio μ_1/μ_2, as would occur for example in an oil/water configuration, the maximum volume flow rate Q_1 is obtained when $a \approx \frac{1}{\sqrt{2}}R$, and is given by

$$\left.\frac{Q_1}{\bar{Q}}\right|_{\max} \approx \frac{1}{2}\frac{\mu_1}{\mu_2}.$$

The volume flow rate of the lower-viscosity fluid is

$$\frac{Q_2}{\bar{Q}} = \frac{\mu_1}{\mu_2}\left(1-\frac{a^2}{R^2}\right)^2.$$

Thus the volume flow rate Q_2 required to maximize Q_1 is

$$\left.\frac{Q_2}{\bar{Q}}\right|_{\max Q_1} = \frac{\mu_1}{\mu_2}\left[\frac{(\mu_1/\mu_2)-1}{2(\mu_1/\mu_2)-1}\right]^2.$$

For large values of μ_1/μ_2 this reduces to

$$\left.\frac{Q_2}{\bar{Q}}\right|_{\max Q_1} \approx \frac{1}{4}\frac{\mu_1}{\mu_2} \quad \text{or} \quad \left.\frac{Q_2}{\bar{Q}}\right|_{\max Q_1} \approx \frac{1}{2}\left(\frac{Q_1}{\bar{Q}}\right)_{\max}$$

4.2. *Evolution of the energy and balance of power of the exterior tractions in the bicomponent flow of immiscible liquids*

The following energy equation due to E. B. Dussan V. governs the flow of immiscible incompressible fluids (for a full discussion see Joseph 1976):

$$\frac{\mathrm{d}}{\mathrm{d}t}\left[\mathscr{E}+\mathscr{P}+\int_\Sigma \sigma\,\mathrm{d}\Sigma\right] = \int_\Sigma \frac{\mathrm{d}\sigma}{\mathrm{d}t}\mathrm{d}\Sigma + \oint_{\partial\Sigma} \sigma\boldsymbol{\tau}\cdot\boldsymbol{U}\,\mathrm{d}l + \int_{\partial\mathscr{V}} \boldsymbol{u}\cdot(\boldsymbol{T}\cdot\boldsymbol{n}) + \int_{\mathscr{V}} \mathrm{tr}\,\boldsymbol{T}\boldsymbol{D}[\boldsymbol{u}]. \quad (4.1)$$

The terms of (4.1) need to be defined and discussed. The definitions of volumes, surfaces, distinguished directions and velocities are defined under figure 3. The stress $\boldsymbol{T}$ is given by (2.1), $\boldsymbol{D}[\boldsymbol{u}]$ is the stretching tensor for $\boldsymbol{u}$,

$\mathscr{E} = \int_{\mathscr{V}} \frac{1}{2}\rho|\boldsymbol{u}|^2$ (kinetic energy),

$\mathscr{P} = \int_{\mathscr{V}} \rho g z$ (potential energy),

$\oint_\Sigma \sigma\,\mathrm{d}\Sigma$ (surface energy),

$\frac{\mathrm{d}\sigma}{\mathrm{d}t}$ (derivative of surface tension following a particle in the surface),

$\oint_{\partial\Sigma} \sigma\boldsymbol{\tau}\cdot\boldsymbol{U}\,\mathrm{d}l$ (power or working of the contact line),

$\int_{\partial\mathscr{V}} \boldsymbol{u}\cdot(\boldsymbol{T}\cdot\boldsymbol{n})$ (power or working of the traction vector $\boldsymbol{T}\cdot\boldsymbol{n}$ on the exterior boundary),

$\int_{\mathscr{V}} \mathrm{tr}\,\boldsymbol{T}\boldsymbol{D}[\boldsymbol{u}]$ (stress power or dissipation).

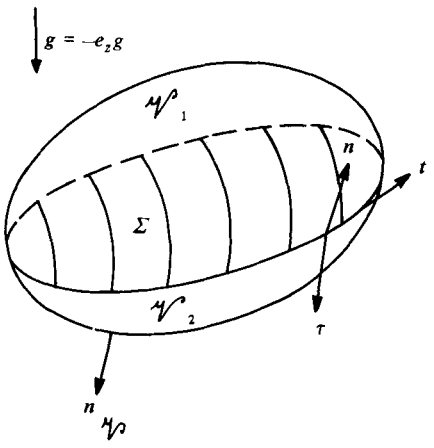

FIGURE 3. Volume, surfaces and distinguished directions for two fluids separated by an interface. $\mathscr{V}_1$ and $\mathscr{V}_2$ are the volumes occupied by the two fluids, $\mathscr{V} = \mathscr{V}_1 \cup \mathscr{V}_2$, $\boldsymbol{n}_i$ is the outward normal to $\partial\mathscr{V}_i (i = 1, 2)$, $\Sigma = \partial\mathscr{V}_1 \cap \partial\mathscr{V}_2$ is the interface separating the two fluids, $\boldsymbol{n}$ is the normal to Σ pointing from $\mathscr{V}_2$ to $\mathscr{V}_1$, $\partial\mathscr{V} = \partial\mathscr{V}_1 \cup \partial\mathscr{V}_2 - \Sigma$ is the exterior boundary; parts of this boundary may be made of rigid solids, $\boldsymbol{n}$ is the outward normal on $\partial\mathscr{V}$, $\partial\Sigma = \Sigma \cap \partial\mathscr{V}$ is the contact line; l is an arclength on this line, $\boldsymbol{t}$ is the tangent vector on $\partial\Sigma$, $\boldsymbol{\tau} = \boldsymbol{t} \wedge \boldsymbol{n}$ is the normal to $\partial\Sigma$ on Σ, $\boldsymbol{u}_i$ is the velocity of the fluid in $\mathscr{V}_i (i = 1, 2)$, $\boldsymbol{U}$ is the velocity of a point of the contact line.

For incompressible Newtonian fluids the dissipation is in the form

$$\int_{\mathscr{V}} 2\mu \operatorname{tr} \boldsymbol{D}^2[\boldsymbol{u}].$$

The steady flow of immiscible fluids satisfies (4.1) with time derivatives set to zero. If $\sigma = 0$, $\boldsymbol{U} = 0$ or if there is no contact line as in some flows of two fluids in pipes or between cylinders, then for Newtonian fluids

$$\int_{\partial\mathscr{V}} \boldsymbol{u} \cdot (\boldsymbol{T} \cdot \boldsymbol{n}) = \int_{\mathscr{V}} 2\mu \boldsymbol{D}[\boldsymbol{u}] : \boldsymbol{D}[\boldsymbol{u}]. \tag{4.2}$$

One selection rule which may be postulated is as follows. *The realized placement of $\mathscr{V}_1$ and $\mathscr{V}_2$ within $\mathscr{V}$ is the one which maximizes the speeds $\boldsymbol{u}$ for prescribed tractions on the exterior boundary $\partial\mathscr{V}$ or minimizes tractions for prescribed speeds.* Joseph, Renardy & Renardy (1984) have shown that this is a well-defined problem with a definite solution in some cases. The selection rule could be stated in terms of fluxes and forces instead of speeds and tractions. The selection rule requires that we first specify a class of variational competitors, say layered Poiseuille flows, before we seek the optimum placements of components. Maximizing speeds is the same as maximizing dissipation for prescribed tractions. Minimizing tractions for given speeds requires that we minimize the dissipation. In Poiseuille flows it is natural to fix the pressure gradient (tractions) and maximize the flux (speeds). In contrast, in Couette flows we specify the speeds (angular velocity) and minimize the shear stresses (torques) at the boundary.

4.3. *Variational problems for Couette flow in plane and circular layers and for layered Poiseuille flow*

Consider layered plane Poiseuille flows of the type shown in figure 4. In general, these flows are uniquely determined up to arrangement. This means that the total number N of layers and the size of the layers, subject to total height constraints, are left

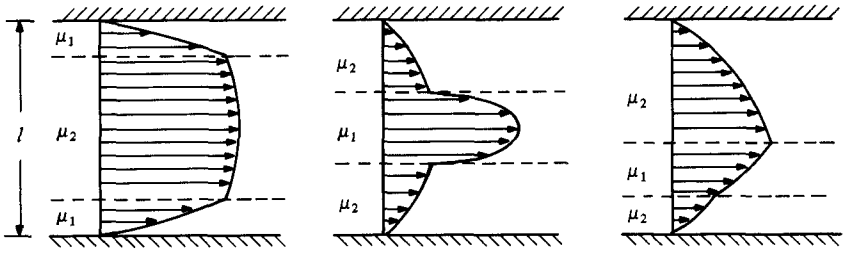

FIGURE 4. Layered plane Poiseuille flow in three layers. The configurations in (*a*) and (*b*) are the centrally located ones. The configuration in (*a*) maximizes the mass flux for a given pressure gradient ($-G$) among the continuum of continguous layers of high-viscosity (μ_2) layers of total height l_2 and low-viscosity (μ_1) layers of total height l_1; $l_1+l_2 = l$.

undetermined. Now we shall write the energy balance (4.2) for layered plane Poiseuille flow. The volume here is a plane area of channel height l and length L (along the axis x). Since $\boldsymbol{u}$ vanishes on the solid walls, the integral on the left of (4.2) is over planes perpendicular to x at x and $x+L$:

$$\int_{\partial\mathscr{V}} \boldsymbol{u}\cdot(\boldsymbol{T}\cdot\boldsymbol{n}) = \int_0^l \left[-uT^{\langle xx\rangle}\Big|_x + uT^{\langle xx\rangle}\Big|_{x+L} \right] \mathrm{d}y$$

$$= (-p_{L+x}+p_x)\int_0^l u\,\mathrm{d}y = -\frac{\Delta p}{L}LQ = GLQ,$$

where $Q = \int_0^l u\,\mathrm{d}y$ is the volume flux. On the other hand

$$2\int \mu \boldsymbol{D}:\boldsymbol{D} = \frac{1}{2}\int \mu u'^2(y)\,\mathrm{d}\mathscr{V}$$

$$= \tfrac{1}{2}L\int_0^l \mu u'^2(y)\,\mathrm{d}y.$$

Hence

$$2GQ = \int_0^l \mu u'^2(y)\,\mathrm{d}y. \tag{4.3}$$

We next recall that between 0 and l are N contiguous layers with fluids of different viscosities. We can suppose that the layer nearest the bottom is occupied by a fluid of viscosity μ_1, the next layer has μ_2, then μ_1 again, and so on. So besides the total number N of layers and their sizes, we need to know if μ_1 is the larger viscosity. We suppose that the total volume (height) of high-viscosity (μ_+) fluid is given as l_+ and l_- is the volume of low-viscosity fluid and $l_+ + l_- = l$. The N layers are divided into intervals

$$[0, y_{(1)}],\ [y_{(1)},\ y_{(2)}],\ [y_{(2)},\ y_{(3)}],\ \ldots,\ [y_{(N-1)}, l].$$

With G given, we maximize

$$Q = \int_0^{y_{(1)}} u_{(1)}(y)\,\mathrm{d}y + \int_{y_{(1)}}^{y_{(2)}} u_{(2)}(y)\,\mathrm{d}y + \ldots + \int_{y(N-1)}^{l} u_{(N)}(y)\,\mathrm{d}y, \tag{4.4}$$

where

$$2QG = \mu_1\int_0^{y_{(1)}} u'^2_{(1)}(y)\,\mathrm{d}y + \mu_2\int_{y_{(1)}}^{y_{(2)}} u'^2_{(2)}(y)\,\mathrm{d}y + \mu_1\int_{y_{(2)}}^{y_{(3)}} u'^2_{(3)}(y)\,\mathrm{d}y + \ldots. \tag{4.5}$$

Now we change variables:

$$\left.\begin{aligned} u_{(1)} &= -\frac{G}{\mu_1} v_{(1)}, \\ u_{(2)} &= -\frac{G}{\mu_2} v_{(2)}, \\ u_{(3)} &= -\frac{G}{\mu_1} v_{(3)}, \end{aligned}\right\} \tag{4.6}$$

where

$$v'_{(n)} = -y + Y \quad (y \in [0, l]) \tag{4.7}$$

satisfies the usual equation for plane Poiseuille flow, $[\![\mu u']\!] = 0$ at each interface, and there is one $Y \in (0, l)$ such that $v'_{(n)}(Y) = 0$. Inserting this change of variables into (4.5), we get

$$\frac{2Q}{G} = \frac{1}{\mu_1}\int_0^{y_{(1)}} (y-Y)^2\,\mathrm{d}y + \frac{1}{\mu_2}\int_{y_{(1)}}^{y_{(2)}} (y-Y)^2\,\mathrm{d}y + \frac{1}{\mu_1}\int_{y_{(2)}}^{y_{(3)}} (y-Y)^2\,\mathrm{d}y + \ldots. \tag{4.8}$$

We maximize this by arranging the layers so that the high viscosity in the denominator is associated with the smallest value of $(y-Y)^2$. This is clearly the arrangement (a) of figure 4, so $N = 3$, and μ_1 is the low-viscosity μ_-.

The same considerations, but in more complicated form, enter into the rigorous solution of this problem for pipe flow given by JRR (1984).

Couette flow differs from Poiseuille flow in that it is perhaps more natural to prescribe the speed of exterior boundaries and to minimize the torque. We first note that for the Couette flow between cylinders in N rings and layers we have

$$\boldsymbol{e}_x \cdot (\boldsymbol{T}\cdot\boldsymbol{n}) = T^{\langle\theta x\rangle} = 0,$$

so that

$$\int_{\partial\mathscr{V}} \boldsymbol{u}\cdot(\boldsymbol{T}\cdot\boldsymbol{n}) = \int_{\partial\mathscr{V}} v(r)\,\boldsymbol{e}_\theta\cdot(\boldsymbol{T}\cdot\boldsymbol{n}) = 2\pi\{b\Omega_2 T^{\langle r\theta\rangle}_{(b)} - a\Omega_1 T^{\langle r\theta\rangle}_{(a)}\} = (\Omega_2 - \Omega_1)\,M, \tag{4.9}$$

where Ω_2 and Ω_1 are the angular speeds of the outer and inner cylinders, and $M = 2\pi r T^{\langle r\theta\rangle}(r)$ is the torque and it is constant for $a \leqslant r \leqslant b$. It is clear from (4.2) that $(\Omega_2 - \Omega_1)\,M$ is positive and that

$$\begin{aligned} M(\Omega_2-\Omega_1) &= \frac{\mu}{2}\int_a^b r^3\left[\frac{\mathrm{d}(v/r)}{\mathrm{d}r}\right]^2 \mathrm{d}r \\ &= \frac{\mu_1}{2}\int_a^{r_{(1)}} r^3\left[\left(\frac{v}{r}\right)'\right]^2 \mathrm{d}r + \frac{\mu_2}{2}\int_{r_{(1)}}^{r_{(2)}} r^3\left[\left(\frac{v}{r}\right)'\right]^2 \mathrm{d}r + \frac{\mu_1}{2}\int_{r_{(2)}}^{r_{(3)}} r^3\left[\left(\frac{v}{r}\right)'\right]^2 \mathrm{d}r + \ldots, \\ \boldsymbol{u} &= \boldsymbol{e}_\theta v(r), \quad [\![p]\!] = 0, \quad \left[\!\!\left[\mu\left(\frac{v}{r}\right)'\right]\!\!\right] = [\![v]\!] = 0 \quad \text{at } r_{(1)}, r_{(2)}, \ldots. \end{aligned} \tag{4.10}$$

We want to choose the arrangements of layers and the placement of viscosities so as to minimize $|M|$ when Ω_2 and Ω_1 are prescribed. It will suffice to solve this problem for a two-layer configuration.

We may always consider the problem posed for two adjacent layers. We find that the minimizing solution has the lower-viscosity fluid on the inside. We conclude that $N = 2$ with more-viscous fluid on the outside and less-viscous fluid inside.

Suppose $r_{(1)} = d$ is the interface between two layers at $r = a$ and $r = b$. The fluid

with viscosity μ_2 occupies the region $a \leqslant r \leqslant d$, and the fluid with viscosity μ_1 occupies the region $d \leqslant r \leqslant b$. We find that in $d \leqslant r \leqslant b$

$$v_1 = A_1 r + B_1/r,$$

$$A_1 = \left\{\mu_2\left(\frac{\Omega_1}{b^2} - \frac{\Omega_2}{d^2}\right) + \mu_1\Omega_2\left(\frac{1}{d^2} - \frac{1}{a^2}\right)\right\}\Big/ q,$$

$$q \equiv \mu_2\left(\frac{1}{b^2} - \frac{1}{d^2}\right) + \mu_1\left(\frac{1}{d^2} - \frac{1}{a^2}\right),$$

$$B_1 = (\Omega_2 - \Omega_1)\,\mu_2/q,$$

and in $a \leqslant r \leqslant d$

$$v_2 = A_2 r + B_2/r,$$

$$A_2 = \left\{\mu_2\Omega_1\left(\frac{1}{b^2} - \frac{1}{d^2}\right) + \mu_1\left(\frac{\Omega_1}{d^2} - \frac{\Omega_2}{a^2}\right)\right\}\Big/ q,$$

$$B_2 = \mu_1 B_1/\mu_2.$$

Since

$$M(\Omega_2 - \Omega_1) = \frac{\mu_2}{2}\int_a^d r^3\left[\left(\frac{v_2}{r}\right)'\right]^2 \mathrm{d}r + \frac{\mu_1}{2}\int_d^b r^3\left[\left(\frac{v_1}{r}\right)'\right]^2 \mathrm{d}r$$

$$= \frac{a^2b^2(\Omega_2 - \Omega_1)^2\,(ka^2 + b^2)\,\mu_1\mu_2}{(b^2 - a^2)\,(b^2\mu_1 + ka^2\mu_2)}, \tag{4.11}$$

where $k = (b^2 - d^2)/(d^2 - a^2)$, is positive, we may, without losing generality, consider the case for which M and $\Omega_2 - \Omega_1$ are positive. It is immediate that $M(k, \mu_1, \mu_2)$ is a monotonically increasing function of μ_2, from zero at $\mu_2 = 0$ to

$$\frac{b^2(\Omega_2 - \Omega_1)^2\,(ka^2 + b^2)\,\mu_1}{(b^2 - a^2)\,k}.$$

It follows from monotonicity that M is larger when $\mu_2 > \mu_1$ than when $\mu_2 < \mu_1$. So we minimize the torque by putting the lower-viscosity fluid $\mu_- = \mu_2$ on the inner cylinder at radius $r = d$.

The situation when one of the liquids occupies an infinite region has to be treated separately. For example, when $b \to \infty$ and $\Omega_2 \to 0$ then

$$|M| = \frac{|\Omega_1|\,a^2d^2\mu_1\mu_2}{(\mu_2 - \mu_1)\,a^2 + \mu_1 d^2}, \tag{4.12}$$

which for a fixed d is smaller when $\mu_2 > \mu_1$.

So in every pair of layers the arrangement that minimizes the torque has the low-viscosity liquid on the inside. It follows that optimal arrangements of layers for minimum torque is the one with two layers and the less viscous fluid on the inner cylinder.

The preferred arrangement for the problem of plane Couette flow in which the velocity is U at $y = l$ and zero at $y = 0$ may be studied using (4.2) in reduced form:

$$UT^{\langle xy\rangle} = \int_0^l u'^2(y)\,\mathrm{d}y. \tag{4.13}$$

It is not hard to verify that the value of the integral on the right of (4.13) is independent of the number and size of layers if the total volume l_+ and l_- of the high- and low-viscosity fluids is prescribed. It follows that the variational problem for the preferred arrangement of layers in plane Couette flow has no solution.

5. Experimental observations of instability configurations

5.1. *Encapsulation instabilities*

We say that a family of steady configurations of components in the flow of immiscible liquids undergoes an encapsulation instability when this family gives way to motions in which the high-viscosity liquid is shielded from shearing by the low-viscosity liquid. This type of instability can be observed as a migration of low-viscosity liquid into regions of high shear. Sometimes the low-viscosity liquid moves into the region of high shear as a sheet, and sometimes (for example when the high-viscosity liquid wets the moving boundary) the low-viscosity liquid fingers into the high-viscosity liquid. Droplets are then torn off the fingers and move into the region of high shear as an emulsion of droplets of low-viscosity liquid in a high-viscosity foam.

The series of experiments described below originated from observations of encapsulation instabilities in pipes. We wanted to know if the theoretical explanation of the observations which involved extremizing dissipation could be defended and extended. We reasoned that minimum dissipation would put low-viscosity liquid on a rotating rod, in the region where there is the greatest shear, as a kind of lubrication bonanza. Though our original idea was known by us to be oversimplified it was definitely useful as a guide to intuition and interpretation.

The experiments were carried out in two rectangular Plexiglas boxes. Each box has a rod inserted through the long planar sides, which is driven by a variable-speed motor. The [length, height, depth, rod diameter, rod composition] of the two boxes I and II respectively are: [20.32 cm, 22.86 cm, 10.16 cm, 5.08 cm, Plexiglas] for I and [20.32 cm, 11.43 cm, 7.62 cm, 2.54 cm, aluminium] for II. A box is filled with the heavier of two liquids up to the central diameter of the rod and the lighter liquid is floated on the top, as in figure 5. Since two liquids are always used the density differences are not vast. The rod is set into steady rotation. We want to know which liquid will coat the rod. The notion that the hydrodynamics will develop so as to minimize the torque, for a given speed, implies that low-viscosity fluid will coat as in figure 6.

The experiments in which we achieved sheet coating of the type described by figure 6 are summarized in table 1. Photographs of 5 entries from table 1 are shown in figures 7–11 (plates 1–3).

5.2. *Rollers*

There are very viscous oils which strongly adhere to certain solid surfaces. For example, high-viscosity ($\mu = 950$ P) silicone oils and polymeric oils such as STP ($\mu = 110$ P) adhere to aluminium and Plexiglas very strongly. When the oils were floated on water the contact angle showed that aluminium favoured water over STP (see figure 12*a*) or over silicone oil (water wets the rod). However, when the rod is made to rotate, it is the oil that coats, and in copious quantities. This is in apparent contradiction of the dissipation principle which, on superficial consideration, would put water on the rod. So we have the impression that contact angles do not tell the whole story about adhesion.

For the very viscous oils the configuration which appears to minimize dissipation is sometimes achieved by a most unexpected configuration which we call rollers. In figure 12(*a*) we show the static configuration in which STP is floated on water. The STP wets the Plexiglas box and water wets the aluminium rod. The rod was put into steady rotation (clockwise in figure 12); it transported all of the STP on the left side of the box (i.e. the upward-motion side of the rod) to the roller of STP, or to a stagnant region of STP on the right (i.e. the downward-motion side of the rod). A thin sheet

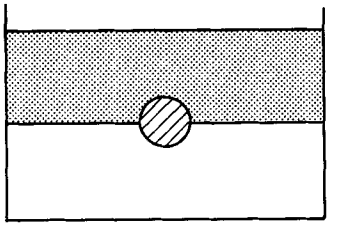

FIGURE 5. The Plexiglas box is loaded with two liquids with the undisturbed interface at the level of the horizontal diameter of the rod.

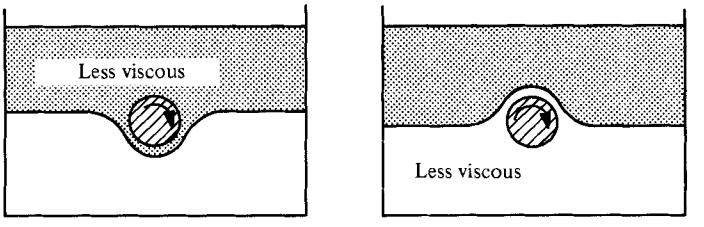

FIGURE 6. The rod rotates and the less viscous liquid coats the rod. This kind of coating is called sheet coating. We say that the low-viscosity liquid encapsulates the high-viscosity liquid because it shields the more-viscous liquid from intense shearing.

of water was pulled between the STP roller and the stagnant STP (see figures 12 and 13). Astonishingly the roller of STP also separated from the wall of the box even though it is well known to us that STP strongly adheres to Plexiglas. This hydrodynamically generated separation of STP from the Plexiglas sidewall is shown in figure 12(*c*).

The STP roller rotates as a rigid wheel, lubricated by water from all sides. The stagnant STP on the right barely moves. A sketch of figure 12 is shown in figure 13 so that there is no ambiguity about what is being shown. This hydrodynamic configuration evidently reduces the total dissipation to a very small value associated mainly with shearing water in a lubrication layer.

Data from experiments leading to rollers is tabulated in table 2.

The rollers are not hard to obtain. They seem to arise out of an encapsulation instability in which the water spontaneously migrates into the regions in which it undergoes high shear, shielding the STP from intense shearing. We have not yet studied the rollers under systematic variations of the parameters. However, in another set of experiments we tried to remove some of the STP from the stagnant region. In fact we removed all but about a 6 mm layer of this STP without visibly affecting the stability of the roller. But, at a critical value of the depth of 'dead' STP, the roller bifurcated into another roller with triangular symmetry. This bizarre triangular 'figure of equilibrium' was unstable but not violently so. In an attempt to save the day we added some STP to the stagnant region and recovered stability. However, the newly stable roller was lopsided and ugly, so we put a screwdriver in the box and moulded it, as does a potter at his wheel, into the automobile-tire shape of large radius which is exhibited in figures 14(*a*, *b*).

The STP rollers are robustly stable. They withstand large perturbations and can rotate for weeks without apparent change.

The development of rollers might be thought to be associated to a degree with normal stresses characteristic of shear flows of non-Newtonian fluids. We discount explanations of our observations based on normal stresses because the shear rates

Liquid 1	Liquid 2	μ_1 (cP)	μ_2 (cP)	ρ_1 (g/cm^3)	ρ_2 (g/cm^3)	Rod wetted by	Rod speed (r.p.m.)	Figure
Silicone I	Glycerol	19	1761	0.96	1.25	Oil	100	8
Silicone I	Water	19	1	0.96	1.0	Oil	~ 150	7(*b*)
Light machine oil	Glycerol	6.36	1761	0.831	1.25	Oil		
Light machine oil	Corn syrup/water	6.36	14	0.831	1.20	Oil		
Silicone I	Corn syrup/water	19	12	0.96	1.20	Oil	~ 150	7(*a*)
Vegetable oil	Glycerol	60	1761	0.92	1.25	Oil		
Castor oil	Glycerol	700	1761	0.96	1.25	Oil	~ 50	9
Water	Dibutyl phthalate	1	18–19	1	1.045	Dibutyl phthalate		
Polyacrylamide (2 % in water)	Dibutyl phthalate	~ 700	18–19	1.02	1.045	Dibutyl phthalate (sheet coating at high speed)		
Castor oil	Polyacrylamide (1 % in water)	700	90	0.96	1.01	Oil (sheet coating at high speed)		
Silicone III	Water	95000	1	0.95	1	Water	~ 65	10, 11

TABLE 1. Experiments in which the low-viscosity fluid coats in sheets

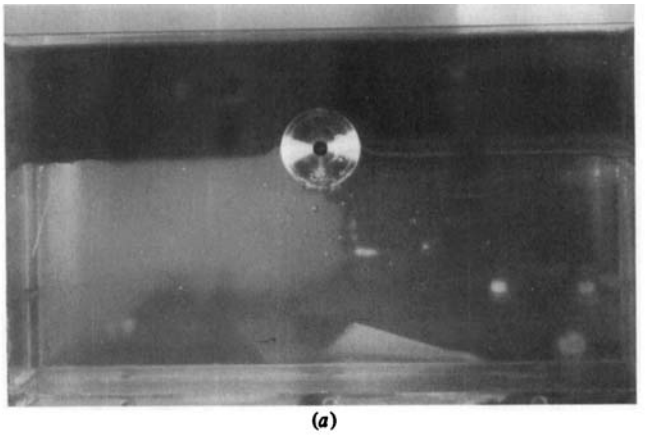

(a)

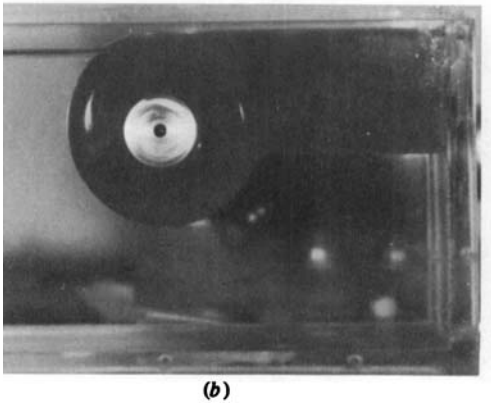

(b)

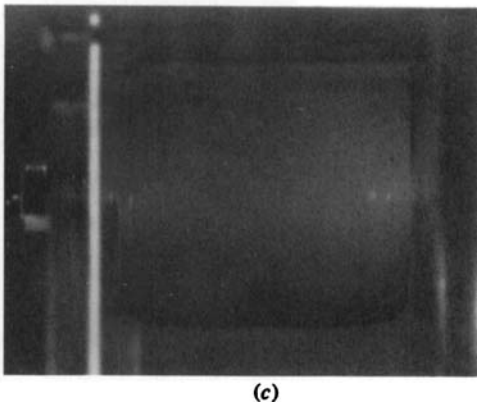

(c)

FIGURE 12. (a) The static configuration of STP (density $\rho = 0.89$ g/cm^3, viscosity $\mu = 11000$ cP, dark) on water ($\mu = 1$ cP). (b) Front view of the box. The rod rotates clockwise at about 40 r.p.m. The STP on the right is nearly stationary and is shielded from shearing by a thin layer of water (c) Side view of the box looking in from the left of (b). The STP roller is also shielded from shearing against the Plexiglas walls by a layer of water.

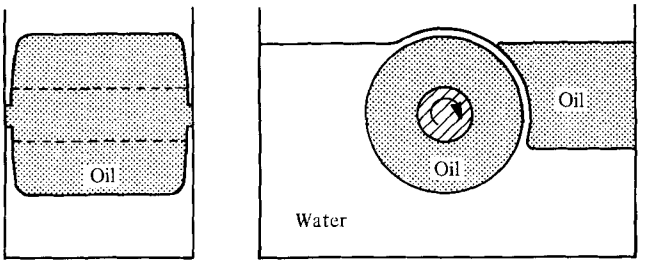

(a) (b)

FIGURE 13. (a) Sketch of figure 12(c); (b) sketch of figure 12(b).

in the rollers appear to be small and because we can obtain rollers in Newtonian liquids.

The photographs exhibited in figure 15 show rollers of silicone oil (950 P) in water. The viscosity ratio is 95000. The roller of silicone oil is almost perfectly round, and it has detached from the walls under hydrodynamic action. The angular velocity of

Liquid 1	Liquid 2	μ_1 (cP)	μ_2 (cP)	ρ_1 (g/cm^3)	ρ_2 (g/cm^3)
STP	Water	11000	1	0.89	1.0
Silicone II	Water	120	1	0.95	1.0†
Silicone III	Water	95000	1	0.95	1.0

† Roller is formed only as a transition and the roller is lopsided.

TABLE 2. Experiments in which the high-viscosity liquid formed rollers lubricated by water

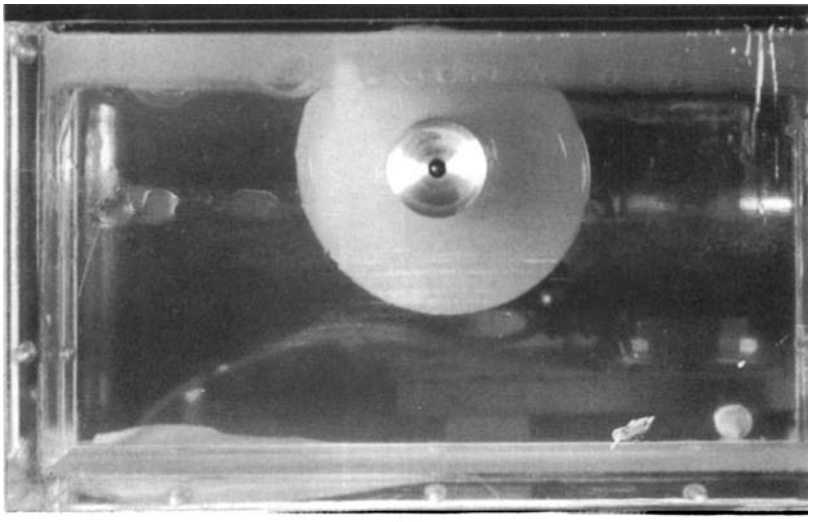

(*a*)

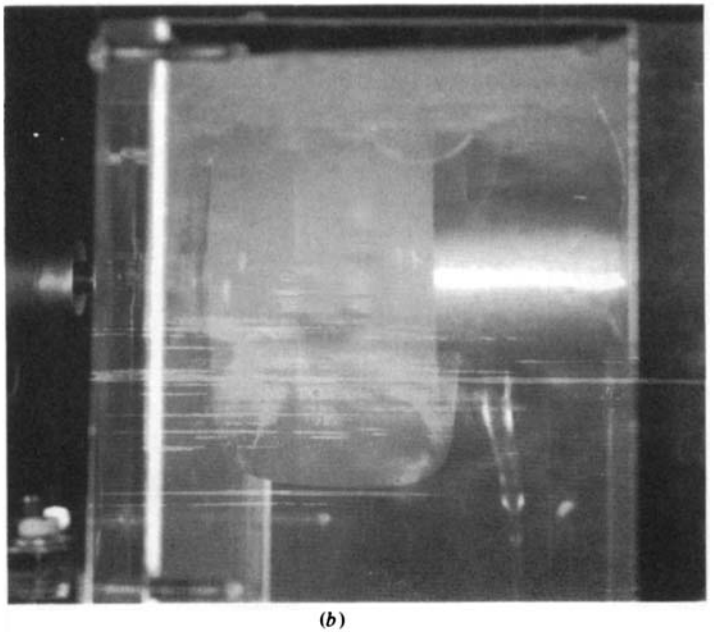

(*b*)

FIGURE 14. (*a*) The same experiment as in figures 12(*b*, *c*) after some STP has been removed from the right of the box, resulting in a roller in the shape of an automobile tire. There is a smaller layer of STP on top of the water. This layer is separated from the roller by a layer of water maintained hydrodynamically. (*b*) Side view of the roller, looking in from the left side of (*a*). The roller has detached from the sidewalls under hydrodynamic action.

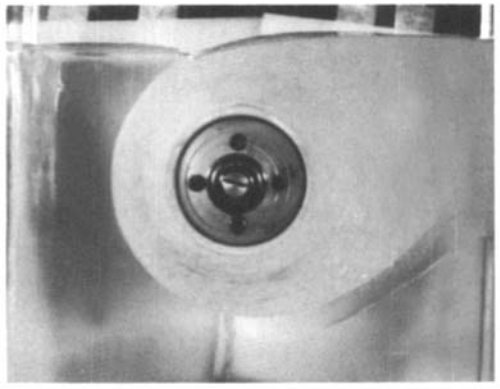

(1)

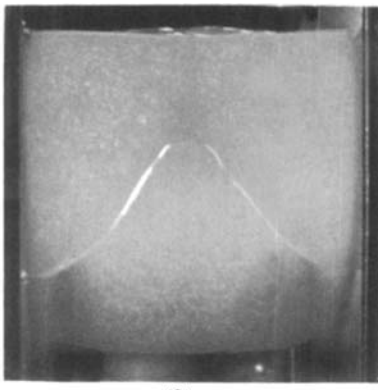

(2)

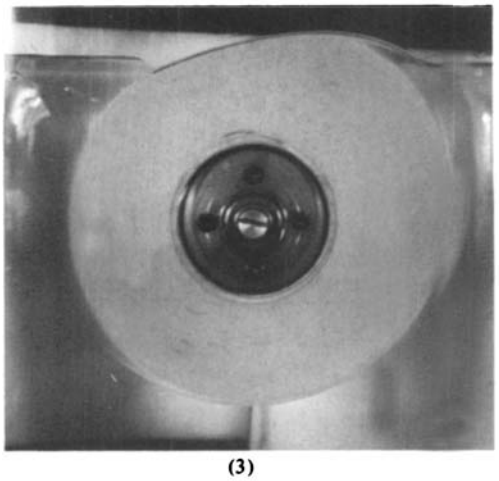

(3)

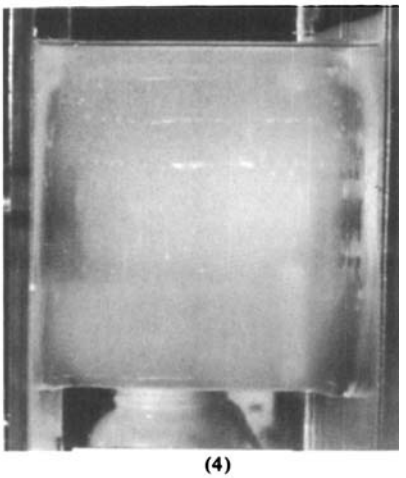

(4)

(a)

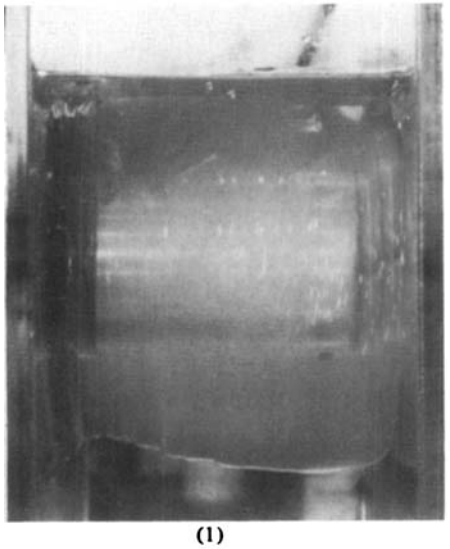

(1)

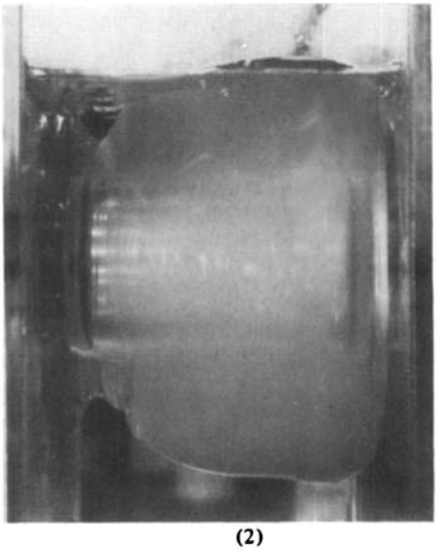

(2)

(b)

FIGURE 15(a, b). For caption see facing page.

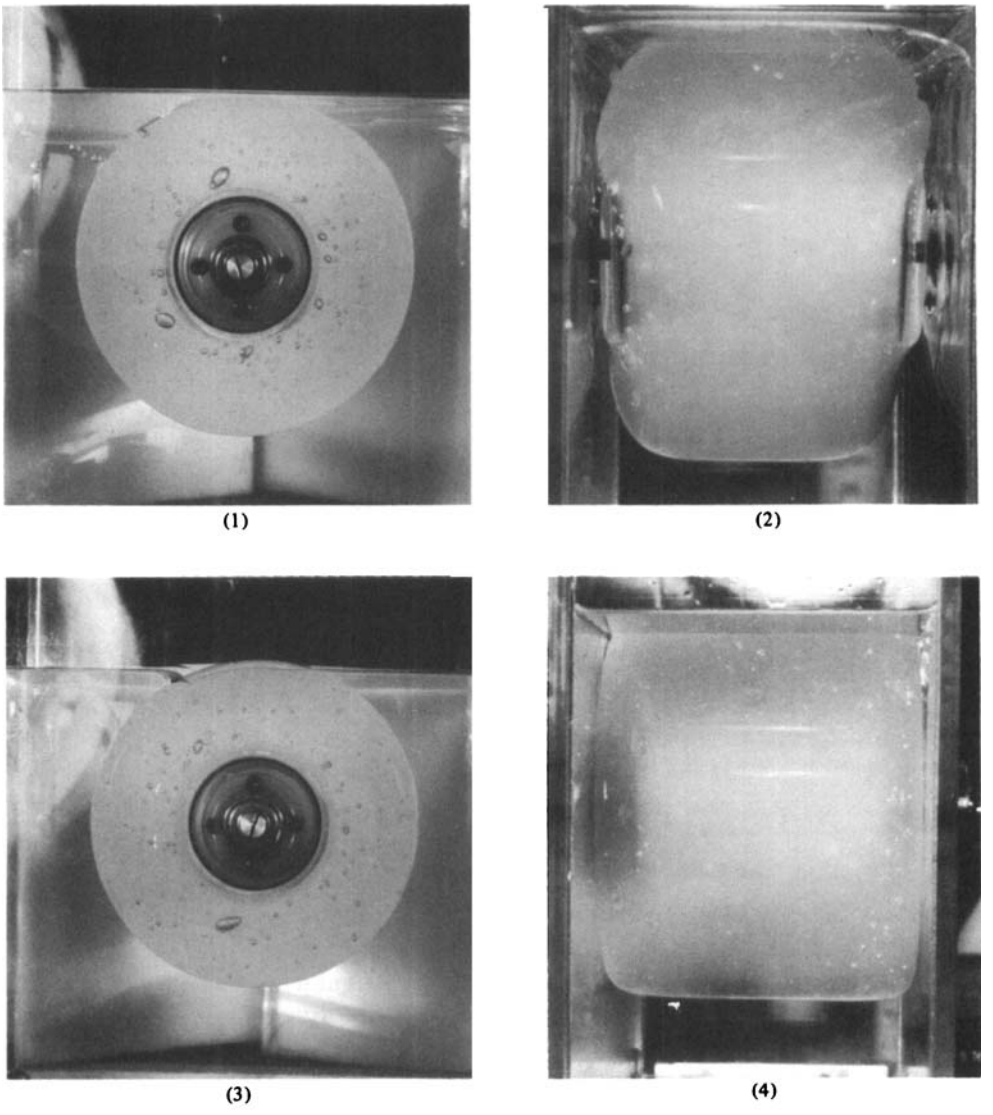

(*c*)

FIGURE 15. (*a*) The formation of a roller of silicone oil III ($\rho = 0.95$ g/cm^3, $\mu = 95000$ cP) in water. In the beginning the rod rotates counterclockwise at 10 r.p.m. The torque is 1.4 lb in. Fingering instabilities lead to an emulsion of water droplets in silicone oil. (1) Front view; (2) side view. Three days later as more water droplets are formed, the effective viscosity of silicone oil decreases and the rod rotates at a higher speed (16 r.p.m.). At this speed the roller is formed but does not rotate as a solid body since it is still attached to the sidewall. (3) Front view; (4) side view. (*b*) The speed of the rod is increased. The torque goes up to above 5 lb in. The two photographs (1) and (2), which are taken 5 s apart, show the dynamics through which the roller detached itself from the sidewall. After detaching from the wall, the torque goes down to 0.6 lb in. (*c*) After detaching from the wall the roller becomes unstable. To restore stability the speed of the rod is reduced to 12 r.p.m. The roller is stable but the shape is irregular. (1) Front view; (2) side view. After a few hours the roller moulded itself into the shape depicted in figure 13. The speed of the rod and the speed on the surface of the roller are almost the same, showing that the roller is very nearly in a solid-body rotation, with small shearing by water at the roller rim.

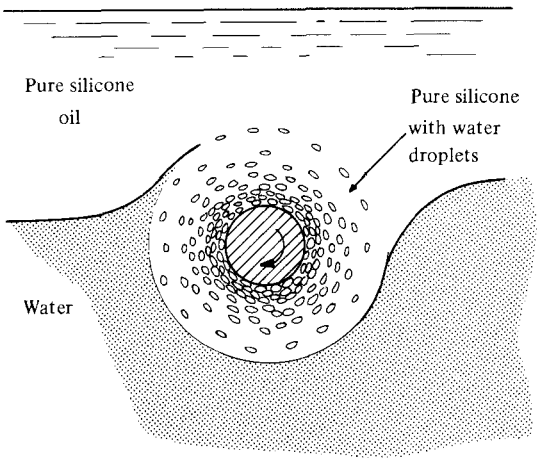

FIGURE 16. Fingering of water droplets into high-viscosity (95000 cP) silicone oil.

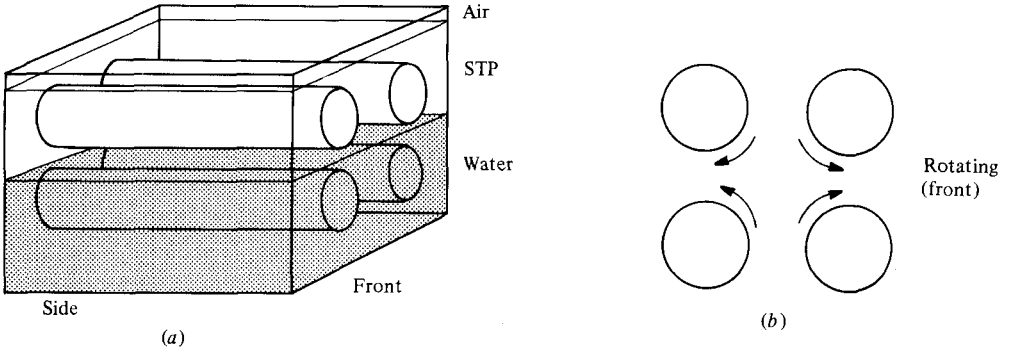

FIGURE 17. Schematic of the experiment with STP and water in the four-roller apparatus.

the silicone roller is constant; the roller rotates as a rigid wheel. The roller is robustly stable, it rotates for weeks without change of form. The dynamics of the roller appears to be governed by the inviscid equations of motion. There is an unknown constant in the pressure which determines the radius of the roller, through the balance of normal stress with surface tension. This radius is not uniquely determined. In fact the roller in figure 15 has captured all of the silicone oil which was originally floated on the water. Presumably if we had floated more or less oil we would achieve a roller with larger or smaller radius. The silicone oil is attracted energetically to the Plexiglas rod; it is favoured over water.

We next describe what happened when we tried to obtain rollers with the same silicone oil ($\mu = 95000$ cP) in the box with an aluminium rod which was wetted by water rather than oil. At first, over a period of about 6 h, we developed an imperfect roller configuration but thereafter we lost the lubricating water film to a cusp-like water film which is characteristic of fingering instabilities and the formation of emulsions (figure 16). The configuration of components then assumed form as a dilute water-laden emulsion of water droplets in silicone oil. The water droplets were continuously generated from the cusp shown in figure 16. The droplets were very effective in reducing the viscosity of the silicone oil. More and more of the water droplets drifted to the rod. After a few days this collection of drops reached a percolation threshold with rings, like wedding bands, of water around the rod. After

three days all the rings had collected into a sheet of water coating the rod and encapsulating the silicone oil. The silicone oil in this configuration appears not to move, though of course there must be some small motion of the silicone oil due to shearing by water. This final configuration is shown in figure 10 (plate 3).

The hydrodynamical history of the silicone-oil experiments exhibits encapsulation phenomena in the form of roller instabilities, fingering instabilities and the generation of emulsions and finally to an unambiguous sheet encapsulation of high-viscosity silicone oil by a lubricating water layer.

The sheet encapsulation can actually be put into a more-dramatic form. In this configuration we get a water layer on the rod, completely surrounded by silicone oil. This was achieved by withdrawing some water with a syringe after the sheet coating with water, described in the previous paragraph, had completely stabilized. The fully encapsulated configuration, shown in figure 11 (plate 3), is robustly stable.†

Arrays of rollers of STP lubricated on all sides by water can be achieved using the four-roller apparatus of G. I. Taylor sketched in figure 17. The apparatus is filled with water up to the plane of symmetry between the upper and lower pairs of rollers, and then STP is added to cover the upper rollers. Rollers of STP (completely surrounded by water) develop out of small sinusoidal disturbances of initially uniform (along rod generators) interfaces; and the water surface between them develops a small wave. The interpenetrating rollers that finally develop are steady, stable and lubricated everywhere by water. Photographs of these rollers are exhibited in figures 18(*a*, *b*) (plate 4). (A grown-up version of the small waviness mentioned above can be seen in figure 18(*a*).)

Figure 18(*c*) (plate 4) shows a top view of interpenetrating rollers of STP and water on two cylinders rotating in opposite directions with the centres of the two cylinders lying in the same horizontal plane. The cylinders are made of steel, and the length of the cylinders and the gap between them can be varied. The cross-section of the STP rollers is roughly square, and is determined by gap size between the cylinders independent of their length. In the case shown, length = 9.5 in., gap = 0.5 in. and cylinder speed $\approx$ 150 r.p.m.

5.3. *Fingering instabilities, the formation of and lubrication by emulsions*

In many cases the wetting properties of the rod or the experimental conditions do not allow the formation of lubricating sheets of low-viscosity liquid. In these cases we get fingering of low-viscosity liquid into high-viscosity liquid. Drops of low-viscosity liquid are torn off the fingertips, leading to the formation of an emulsion of low-viscosity drops in a high-viscosity foam. A type of capillary instability may be associated with drop formation from fingers. The emulsions have a very low viscosity and they shield the bulk of high-viscosity liquid from shearing. In table 3 we have summarized the experiments exhibiting fingering into emulsions.

The first group of emulsifying configurations are those in which a light liquid of moderately high viscosity, like vegetable oil, light machine oil or castor oil, is floated on top of water, or waterbased polymeric solutions, like polyacrylamide. In all these cases the oil wets the Plexiglas rod, and, after the whole rod is exposed to oil, the oil clings tenaciously to the rod in a narrow layer, even in a monolayer, in apparent but

† It is possible to obtain a water-lubricated aluminium rod in which the thickness of the water layer is zero, confined to a monolayer on the rod. In such configurations the rod rotates at high speeds, but the silicone oil is dead still. This violates the no-slip condition; it slips, completely as in an inviscid fluid. So if we wish to say that fluid will stick to a solid we must specify the fluid, the solid, and say there are no monolayers, or make other quantifying statements.

Liquid 1	Liquid 2	μ_1 (cP)	μ_2 (cP)	ρ_1 (g/cm^3)	ρ_2 (g/cm^3)	Rod wetted by
Vegetable oil	Water	60	1	0.92	1.0	Oil
Peanut oil	Water	60	1	0.92	1.0	Oil
Castor oil	Water	700	1	0.96	1.0	Oil
Light machine oil	Water	6.36	1	0.831	1.0	Oil
Castor oil	Polyacrylamide (1 % in water)	700	90	0.96	1.01	Oil, emulsion at low speed
STP	TLA 227	11000	20000	0.89	0.895	STP
STP	Polyacrylamide (1 % in water)	11000	90	0.89	1.01	Polyacrylamide
STP	Water	11000	1	0.89	1.0	Water
Polyacrylamide (2 % in water)	Dibutyl phthalate	700	19	1.02	1.045	Emulsion at low speed

TABLE 3. Experiments in which the low-viscosity fluid coats by fingering in emulsions

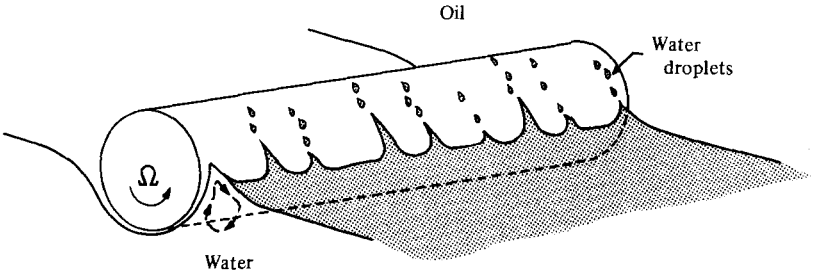

FIGURE 20. Fingering instability leading to emulsions of water droplets in oil foam.

only superficial contradiction of the lubrication principle. When the rod rotates slowly there is a tendency for water to be drawn up onto the rod, but surface tension pulls the water back as shown in figure 19(*a*) (plate 5). The contact angle in this experiment seems to be fixed with the contact line slipping on the rod in such a way as to stay fixed in space. The configuration of the contact line and the tenacity of the contact angle even under pressure from the intense water circulation under the free surface are noteworthy. At a higher speed the water will begin to finger into the oil, depositing droplets as shown in figure 19(*b*). The fingering instability is sketched in figure 20. The continuous formation of droplets leads eventually to emulsification of water droplets in oil foam. The emulsified liquid then coats the rod as shown in figure 19(*c*). Instead of sheet coating we get coating by water-laden emulsions. These emulsions have very low viscosities; first they are water-laden; secondly, they tank-tread like roller bearings, and they seem to be nearly as effective as sheet coats in shielding the high-viscosity liquids from shearing.

The photograph of castor oil ($\mu = 700$ cP, $\rho = 0.96$ g/cm^3) above 1 % polyacrylamide/water ($\mu = 90$ cP, $\rho = 1.01$ g/cm^3) shown in figure 21 (plate 6) is a variant of fingering dynamics leading to drops and emulsions. In this, the rod (rotating at 1 r.p.m.) is covered by polyacrylamide/water droplets, and these droplets in turn are encapsulated at higher speed by a sheet of low-viscosity (polyacrylamide/water) liquid, which shields them from shearing against the high-viscosity castor oil.

A second group of emulsifying configurations is generated by experimental conditions which prevent the generation of sheet coating. We did some experiments in box II of the type that led to the formation of the rollers shown in figures 12(*a–c*). The only difference was that the box was filled to the top and kept from moving there by a cover plate. We expected that the phase configuration of minimum dissipation would lead to the capture of low-viscosity fluid on the rod, with most of it on the rod if the densities were nearly matched. The difference between this sequence of experiments and the ones in §5.2 is that the cover plate forces a kind of hydrodynamic lubrication at the top of the cylinder, promoting fingering and the formation of emulsions.

Realizations of the idea of the foregoing paragraph are shown in figures 22(*a*, *b*) (plate 6). As always, we started with the static configuration of heavy fluid below as shown in figure 12(*a*). In figure 22(*a*) we see the phase configuration of STP ($\mu = 11000$ cP, $\rho = 0.89$ g/cm^3) and TLA 227 ($\mu = 20000$ cP, $\rho = 0.895$ g/cm^3) after a few days with the rod rotating clockwise at about 16 r.p.m. Both fluids are oil-based polymeric immiscible liquids. The density of TLA 227 is about 0.005 g/cm^3 greater than the density of STP. It can be seen in figure 22(*a*) that after a few days much of the STP had migrated to the rod, and the streamlines carrying in the STP from remote regions are evident. When the (dark) STP is drawn from remote regions to

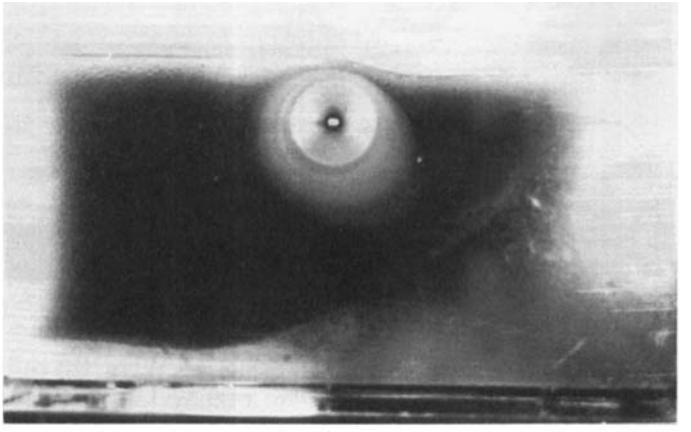

(a)

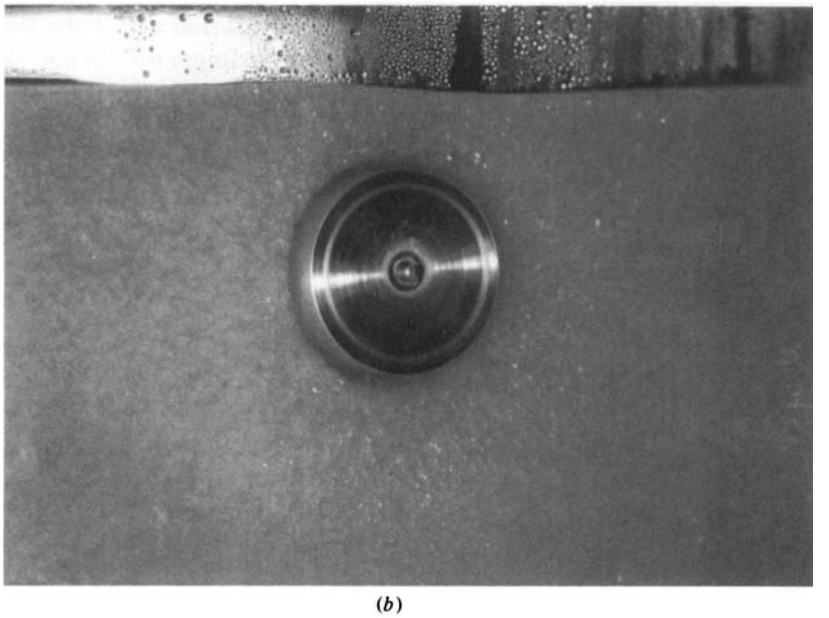

(b)

FIGURE 23. (a) Emulsion of 1% polyacrylamide/water ($\mu = 90$ cP, $\rho = 1.01$ g/cm^3) in STP ($\mu = 11000$ cP, $\rho = 0.890$ g/cm^3, dark). The polyacrylamide/water solution is on the bottom and on the rod, which rotates clockwise at about 45 r.p.m. (b) Close-up view showing the emulsion and the ring of polyacrylamide/water solution around the rod.

the rod it carries with it some (light) TLA 227 by shearing action. After a week the colour differences were very faint and we were unsure if the bulk of the STP was really on the rod. But when we stopped the rod the STP precipitated out, as illustrated in figure 22(b).

The shielding effect of emulsions is very clearly seen in the experiment with STP (dark) above polyacrylamide in water (clear), shown in figures 23(a, b). The polyacrylamide is heavy and much less viscous (viscosity ratio of 120). The STP has a great affinity for the rod, and when we turned on the rod it pulled along a big annulus of the high-viscosity STP, going against our idea that the low-viscosity fluid coats. But after a while the small bubbles of polyacrylamide which were being torn off were

injected into the STP and the whole of the STP emulsified after about three days. The parts of the emulsion having a heavier concentration of low-viscosity polyacrylamide drifted to the rod and all the shearing was confined to the low-viscosity emulsion near the rod. Then the polyacrylamide in the emulsion near the rod was deposited in almost pure form onto the rod. This appears as a light ring of polyacrylamide on the rotating rod shown in figure 23(*b*). The bulk of the STP is completely quiescent, being shielded from the polyacrylamide by the emulsion. We think that this configuration very nearly minimizes dissipation, but we did not anticipate that the hydrodynamics would take on such bizarre forms. The rotational speed appeared to have increased a lot (at the same torque) in the week and one half of rod turning, suggesting a big drop in the dissipation of the preferred phase configuration.

5.4. *Centrifugal and Taylor-type instabilities in the flow of immiscible liquids*

The instabilities we have in mind are the ones which are commonly associated with an adverse distribution of angular momentum. For single fluids such instabilities are well understood in certain circumscribed circumstances; Taylor cells are the best known and most important example. The point of novelty here is the presence of two liquids. Two types of phenomena that occur in our experiments are of interest. The encapsulation instability seems always to position a low-viscosity film or emulsion between the rod and a stagnant body of high-viscosity liquid. Such a configuration is very conducive to the development of an adverse distribution of angular momentum. The tendency for centrifugal forces to throw the heavy, less-viscous liquid outward seems to be resisted by the other more-viscous and still stable portion of the fluid. This type of dynamics may be involved in the flow shown in figure 24. On the other hand the free surface shown in figure 24 is not so unlike the ones exhibited by Moffatt (1977) in his study of viscous films on the outer surface of a rotating cylinder.

A second type of phenomenon develops in the flow of immiscible liquids in a Taylor apparatus set on its side. The inner diameter of the outer cylinder is 6.35 cm, and the length of the space between the inner and outer cylinders is 30.48 cm. The cylinders are made of Plexiglas, the outer is stationary and the inner is free to rotate. Three inner cylinders (diameter = 5.72, 5.08, 3.81 cm) were used in the experiments. Every experiment was carried out with equal volumes of the two liquids. The apparatus was half-filled with heavy liquid on the bottom and light liquid on the top as in figure 25(*a*).

The fluid dynamics of the resulting flow is dominated by a form of Taylor instability which seems to be only weakly influenced by gravity. An idealized sketch of the cells which develop is shown in figure 25(*b*). High- and low-viscosity cells (e.g. oil and water) separate each other. Examples of the cells that actually do develop are exhibited in figures 26–30 (plates 7 and 8).

Figure 26 shows rollers of silicone oil I ($\rho = 0.95$ g/cm^3, $\mu = 19$ cP) separating Taylor cells of water; here $\Omega = 130$ r.p.m., with $R_2 - R_1 = 0.635$ cm. The azimuthal velocity of silicone oil is much larger than water, presumably because of encapsulation by a thin film of water (see figure 32). In figure 27 the rod is rotating at a much higher angular velocity $\Omega = 1810$ r.p.m., with $R_2 - R_1 = 0.318$ cm. At this velocity the oil and water are both unstable and the oil has completely emulsified, forming a single liquid in which we see classical Taylor cells. Figure 28 shows rollers of STP separating Taylor cells of water; here $\Omega = 86$ r.p.m., $R_2 - R_1 = 1.27$ cm. The viscosity of the STP is 11000 times that of water, so that STP is always stable against Taylor instability. The azimuthal velocity of the rollers is much greater than that of the wave

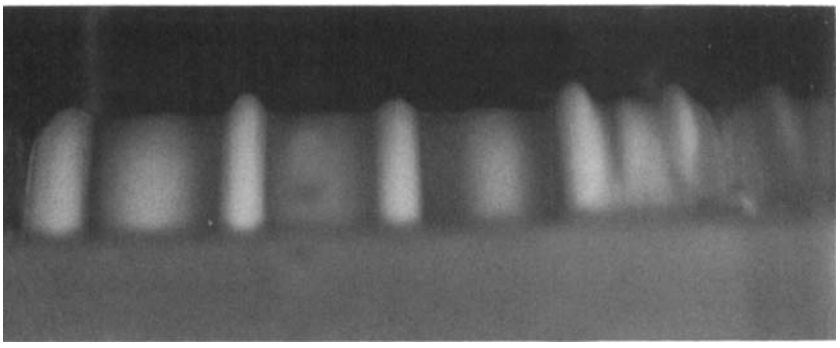

FIGURE 24. Centrifugal instability of multigrade motor oil (10W40) in water. The layer of oil on the rod is separated from the main body of oil by a sheet of water. At the speed of about 300 r.p.m. the oil–water interface becomes wavy.

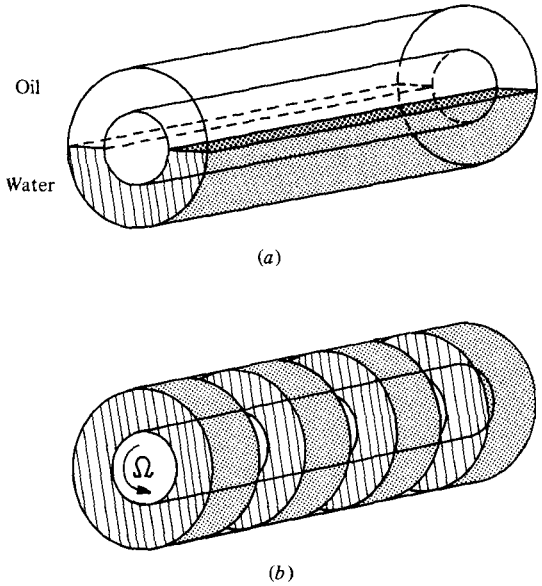

FIGURE 25. Sketch of Taylor cells developing from the instability of water. The oil is dynamically passive while the motion in the water is driven by centrifugal instability.

of STP which sticks to the inner wall of the outside cylinder above the water (see figures 31*c*, 32). The manner in which the STP is fractured to avoid being sheared is noteworthy. Figures 29 and 30 show monograde motor oil (SAE 40) and water, with $R_2 - R_1 = 0.318$ cm. In figure 29, $\Omega = 120$ r.p.m.: at this speed only water is unstable, and the dynamics is similar to figure 31 (*c*). We see rollers of oil separating Taylor cells of water. The azimuthal velocity of water is much smaller than that of oil, apparently caused by the layers of oil sticking to the inner wall of the outer cylinder. With a higher $\Omega = 440$ r.p.m. we see the phenomenon shown in figure 30. This is like a two-component flow of two different emulsions, and the dynamics which are realized seem to fall under figure 31 (*b*).

Encapsulation instabilities enter into the dynamics of the cells shown in figures 26–30 in an important way which we specify below.

It is a good idea to compute stability limits for centrally located Couette flows of immiscible liquids in two layers with gravity neglected. This type of calculation would

lead to critical conditions for the appearance of cells. For the present we imagine that there is a critical Taylor number, which is given by analysis for one fluid and is in the form

$$T_c = \frac{4\Omega^2 R_1^4}{\nu^2} \frac{\eta^2}{1-\eta^2} \frac{(1-\eta)^4}{\eta^4},$$

where R_1 is the radius of the inner cylinder, R_2 is the radius of the outer cylinder, $\eta = R_1/R_2$, ν is the kinematic viscosity and Ω is the angular velocity of the inner cylinder. For small $1-\eta = \epsilon$, $T_c = 3416$ and

$$3416 = \frac{2\Omega^2 R_1^4}{\nu^2} \epsilon^3.$$

In the experiments shown in the photographs exhibited in this paper the liquid with the smaller viscosity is water with $\nu = 0.01$ St. We may estimate $\epsilon = 1-\eta$ for the water alone as

$$\epsilon = \frac{1}{2}\left(1 - \frac{R_1}{R_2}\right).$$

Then, as a rough measure of critical conditions we have

$$\Omega_c = \frac{\sqrt{1708}}{100 R_1^2}\left[8\left(\frac{R_2}{R_2 - R_1}\right)^3\right]^{\frac{1}{2}}.$$

This is an estimate of the critical speed in water. The critical speed for oil is higher; roughly $20\Omega_c$ for silicone oil I ($\mu = 19$ cP), and $12000\Omega_c$ for STP ($\mu = 11000$ cP).

At low speed, we see at first a high torque, which very rapidly drops to a lower value. Correlating this with direct observation, we identify the first significant dynamical event as an encapsulation instability in which a sheet of water is pulled around the inner cylinder. After this event, gravity seems less important and the flows tend more to axisymmetry.

The next event is the formation of Taylor cells in the water layer. The dynamics associated with this event are not perfectly understood in detail but probably can be roughly described as follows. Imagine that a layer of water occupies the region next to the inner cylinder, with $[\![\rho]\!] = 0$ or, equivalently, $g = 0$. As Ω is increased past criticality, the smooth flow of water gives up stability to Taylor vortices. The oil also moves very slowly in cells, driven not by instability but by shear stresses induced by cellular motion of the dynamically active water. These motions will naturally distort the oil/water interface, as in figure 31 (*a*). The large-amplitude limit of the flow in figure 31 (*a*) is usually like the flow depicted in figure 31 (*c*). In this flow the passive oil cells undergo extremely weak cellular motions driven by shears from active water cells. The oil cells are rollers, and are lubricated at the sides and at the outer cylinder by water. The lubrication of oil rollers by water is enhanced by the fact that water is heavier than oil and will tend to replace the oil layer on the outside of the cylinder. If the oil has a strong adhesion to Plexiglas a small layer of oil will continue to adhere to the outer cylinder at positions above the water layer where the shears are small. To understand that it is necessary to study figure 32. In the experiments it is very easy to see that the azimuthal component of velocity of oil cells near the outer cylinder is much greater than the azimuthal component of velocity in neighbouring water cells. This striking observational fact is completely explained by the encapsulation of the oil rollers by water at the outer wall.

When the viscosity of the oil is not too great, it is possible to run our apparatus

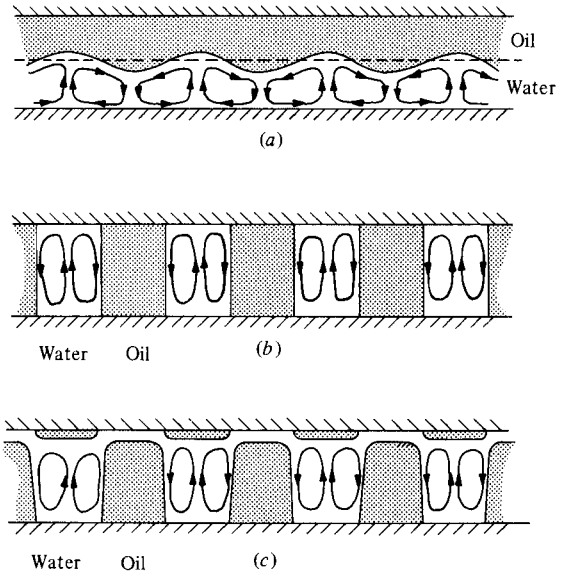

FIGURE 31. Sketch of dynamically active water cells and dynamically passive oil cells (shaded) arising from the instability in bicomponent Couette flow between rotating cylinders. The situation in (*a*) arises near criticality as an instability of layered Couette flow. The situation in (*b*) could be regarded as the large-amplitude limit of (*a*) when density differences are negligible. The secondary flow in the oil cells is extremely weak. Instead of (*b*) we usually see a configuration like (*c*) with passive oil cells rotating as rigid rollers attached to the inner cylinder and lubricated by water at the outer cylinder.

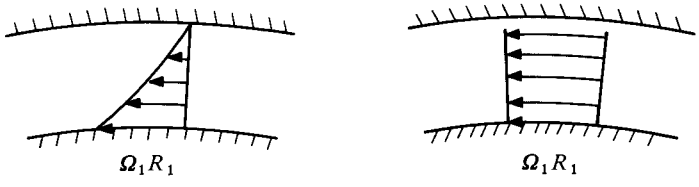

FIGURE 32. The azimuthal velocity distribution in (*a*) water cells, and (*b*) oil rollers lubricated by water.

at speeds for which both oil and water are very unstable to Taylor vortices. In such situations the two components emulsify strongly, forming one emulsified liquid which exhibits Taylor cells in classical form (see figure 27).

This work was supported by the U.S. Army Research Office and by the National Science Foundation.

REFERENCES

BUSSE, F. H. 1982 Multiple solutions for convection in a two component fluid. *Geophysical Res. Lett.* **9**, 519.

CHARLES, M. E. & REDBERGER, P. J. 1962 The reduction of pressure gradients in oil pipelines by the addition of water: numerical analysis of stratified flow. *Can. J. Chem. Engng* **40**, 70.

EVERAGE, A. E. 1973 Theory of stratified bicomponent flow of polymer melts. I. Equilibrium Newtonian tube flow. *Trans. Soc. Rheol.* **17**, 629.

HASSON, D., MANN, U. & NIR, A. 1970 Annular flow of two immiscible liquids. I. Mechanisms. *Can. J. Chem. Engng* **48**, 514.

HOOPER, A. P. & BOYD, W. G. C. 1983 Shear-flow instability at the interface between two viscous fluids. *J. Fluid Mech.* **128**, 507.

JOSEPH, D. D. 1976 *Stability of Fluid Motions II.* Springer.

JOSEPH, D. D., RENARDY, M. & RENARDY, Y. 1984 Instability of the flow of immiscible liquids with different viscosities in a pipe. *J. Fluid Mech.* **141**, 309.

LEE, B. L. & WHITE, J. L. 1974 An experimental study of rheological properties of polymer melts in laminar shear flow and of interface deformation and its mechanisms in two-phase stratified flow. *Trans. Soc. Rheol.* **18**, 467.

MACLEAN, D. L. 1973 A theoretical analysis of bicomponent flow and the problem of interface shape. *Trans. Soc. Rheol.* **17**, 385.

MINAGAWA, N. & WHITE, J. L. 1975 Coextrusion of unfilled and TiO_2-filled polyethylene: influence of viscosity and die cross-section on interface shape. *Polymer Engng Sci.* **15**, 825.

MOFFATT, H. K. 1977 Behaviour of a viscous film on the outer surface of a rotating cylinder, *J. Méc.* **16**, 651.

PLATEAU, J. A. F. 1873 *Statique Expérimentale et Théorique des Liquides.* Gauthier-Villars.

SOUTHERN, J. H. & BALLMAN, R. L. 1973 Stratified bicomponent flow of polymer melts in a tube. *Appl. Polymer Sci.* **20**, 175.

WILLIAMS, M. C. 1975 Migration of two liquid phases in capillary extrusion: an energy interpretation. *AIChE J.* **21**, 1204.

YIH, C. S. 1967 Instability due to viscosity stratification. *J. Fluid Mech.* **27**, 337.

YU, H. S. & SPARROW. E. M. 1967 Stratified laminar flow in ducts of arbitrary shape. *AIChE J.* **13**, 10.

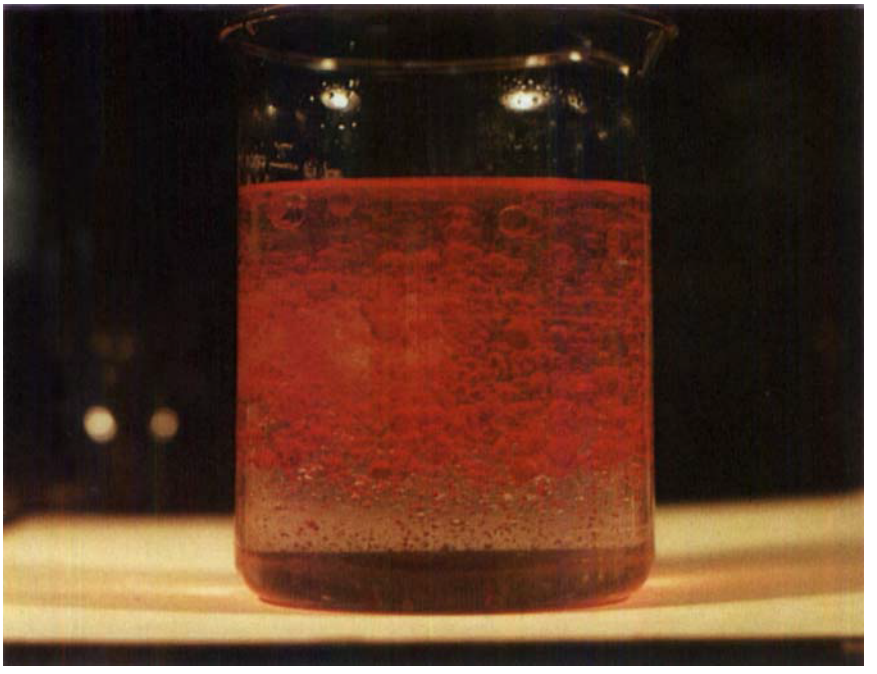

FIGURE 1. One of the static configurations of dibutyl phthalate bubbles in glycerol/water solution.

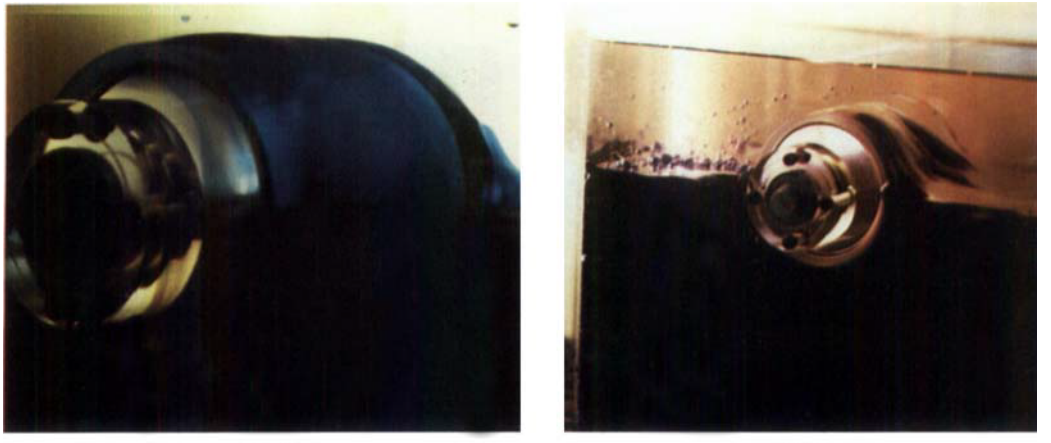

FIGURE 7. Encapsulation of silicone oil I by *(a)* corn syrup/water solution (blue); *(b)* water (blue).

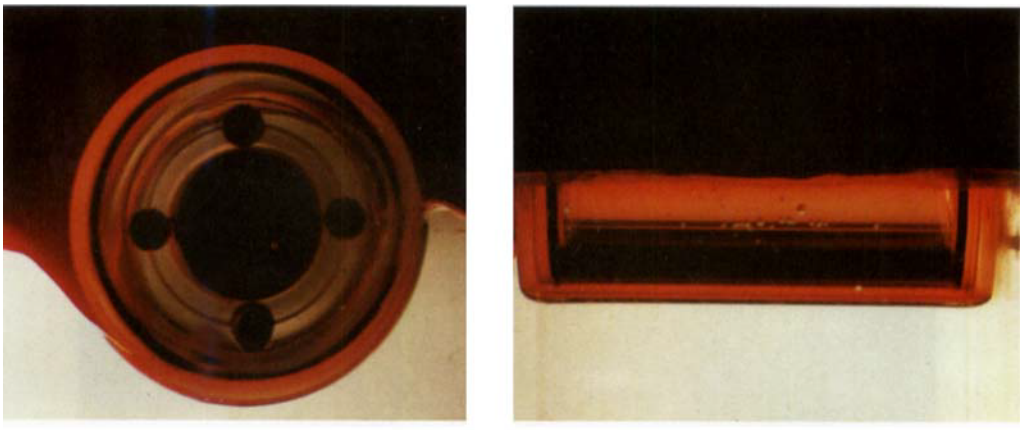

FIGURE 8. Encapsulation of glycerol (clear) by silicone oil I (red): *(a)* front view; *(b)* side view.

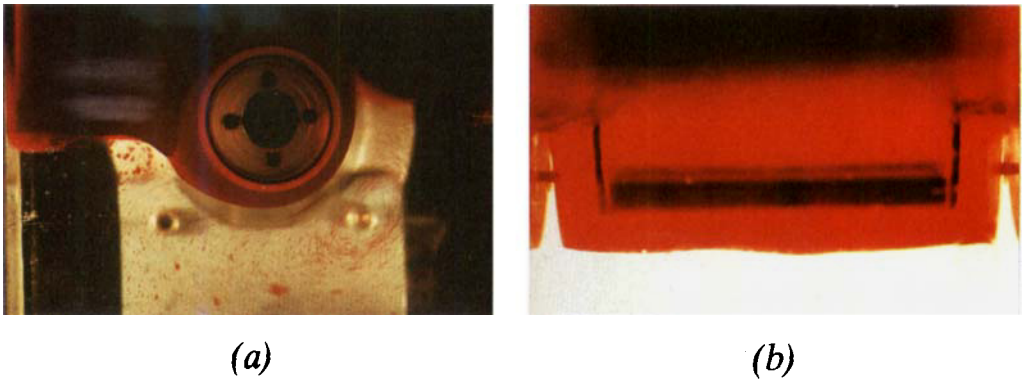

FIGURE 9. Encapsulation of glycerol (clear) by castor oil (red): *(a)* front view; *(b)* side view.

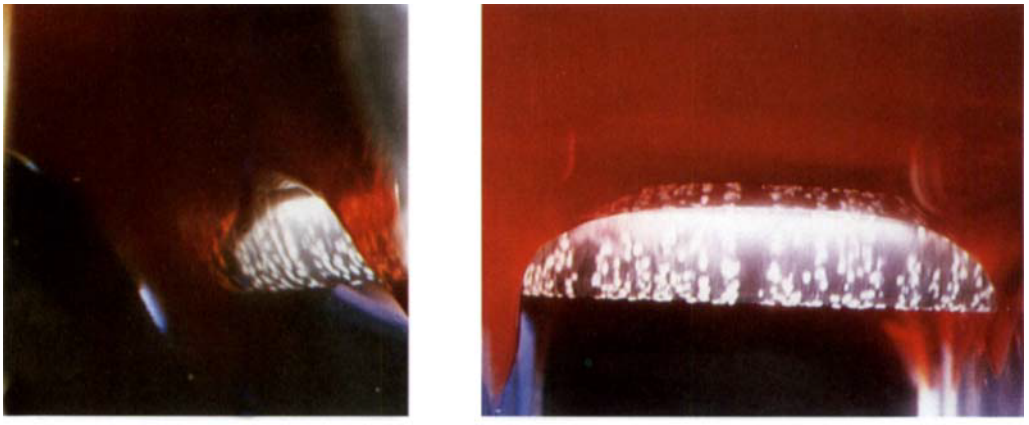

FIGURE 10. Encapsulation of silicone oil III (red) by water (clear): *(a)* back view, looking at an angle from below; *(b)* side view.

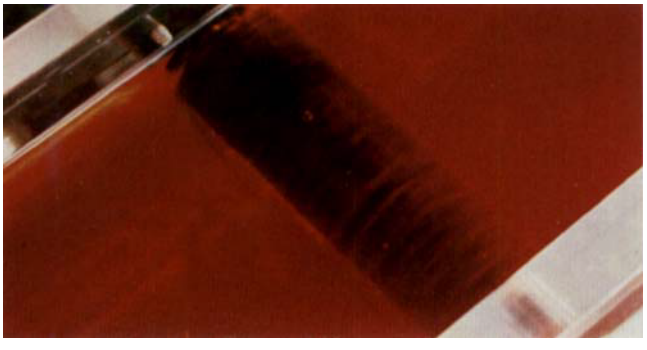

FIGURE 11. The same experiment as in figure 10, but with the silicone level below the rod.

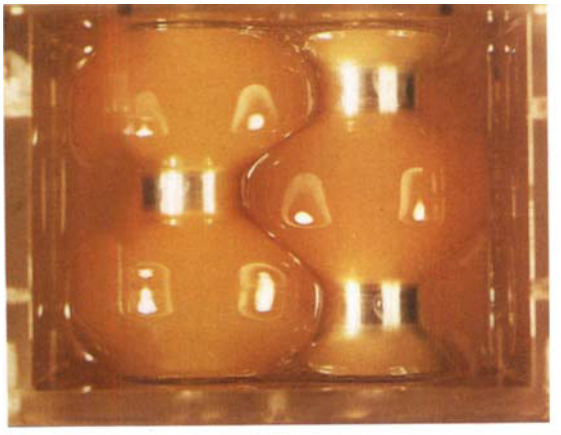

(a)

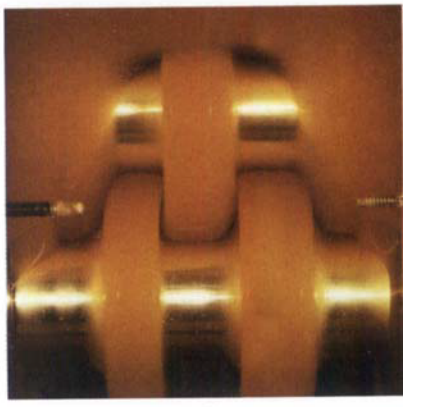

(b)

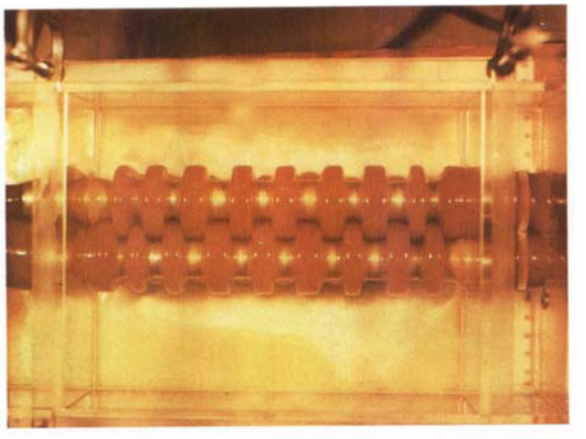

(c)

FIGURE 18 *(a,b)*. Interpenetrating rollers of STP and water in a 4-roller apparatus: *(a)* top view; *(b)* side view (the clear parts are water). *(c)* Interpenetrating rollers on two cylinders rotating in opposite directions.

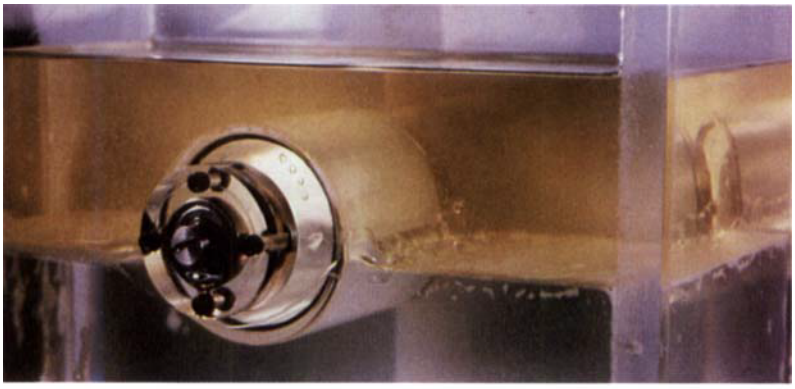

(a)

(b)

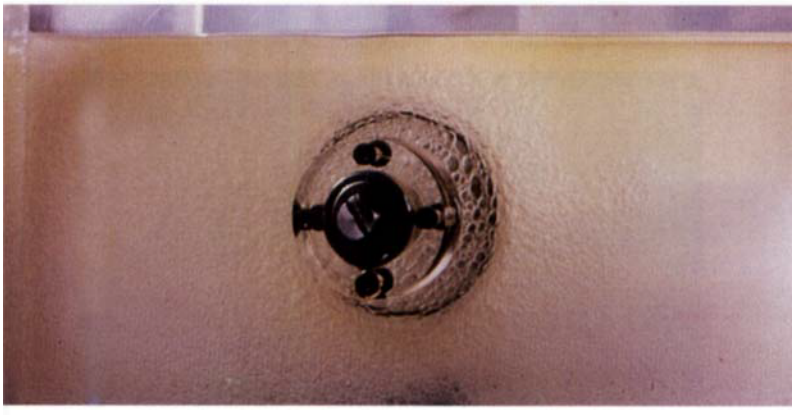

(c)

FIGURE 19. Light machine oil (ρ = 0.831 g/cm^3, μ = 6.36 cP, yellow) on water. *(a)* Rod rotates counterclockwise at 115 r.p.m. *(b)* Rod rotates at 195 r.p.m. *(c)* Emulsion of water in light machine oil at 300 r.p.m.

FIGURE 21. A combination of emulsion and sheet coating of 1% polyacrylamide/water (blue) in castor oil (yellow).

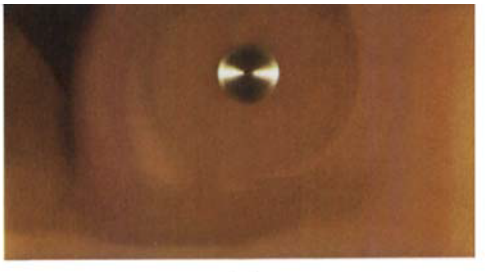

(a)

(b)

FIGURE 22. *(a)* Emulsion of STP (dark brown) in TLA 227 (light brown). *(b)* Emulsion of STP in TLA 227.

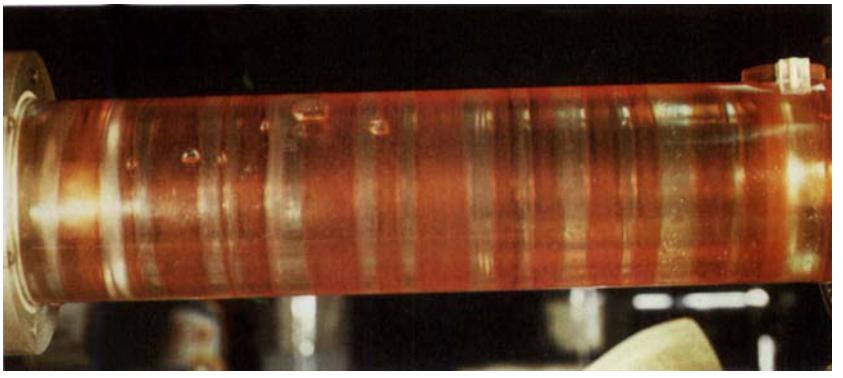

FIGURE 26. Rollers of silicone oil I (red) separating Taylor cells of water (clear).

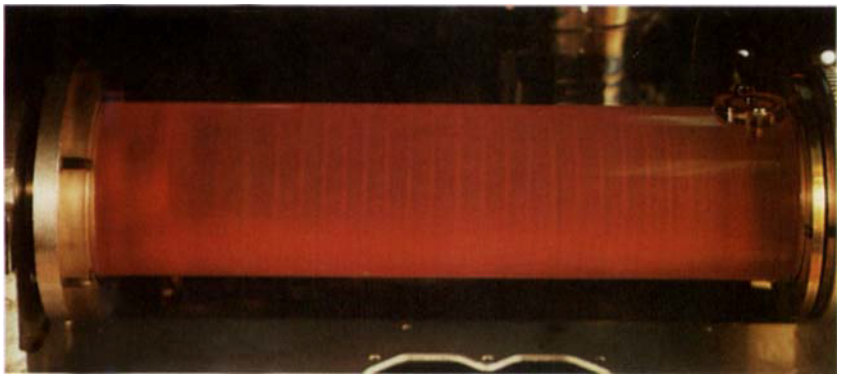

FIGURE 27. As in figure 26, but with much higher angular velocity.

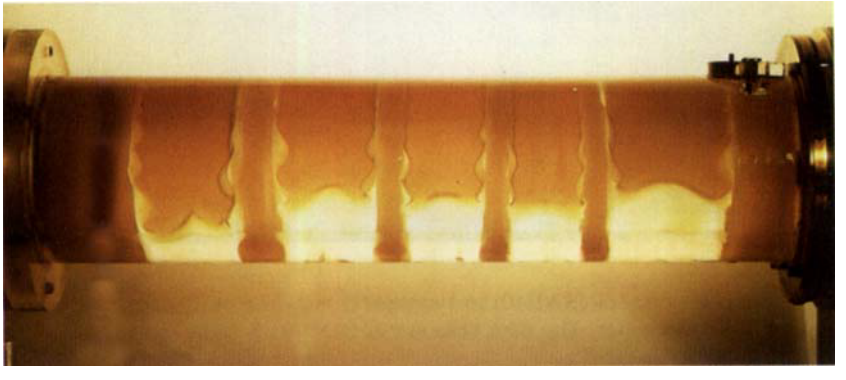

FIGURE 28. Rollers of STP (orange) separating Taylor cells of water (clear).

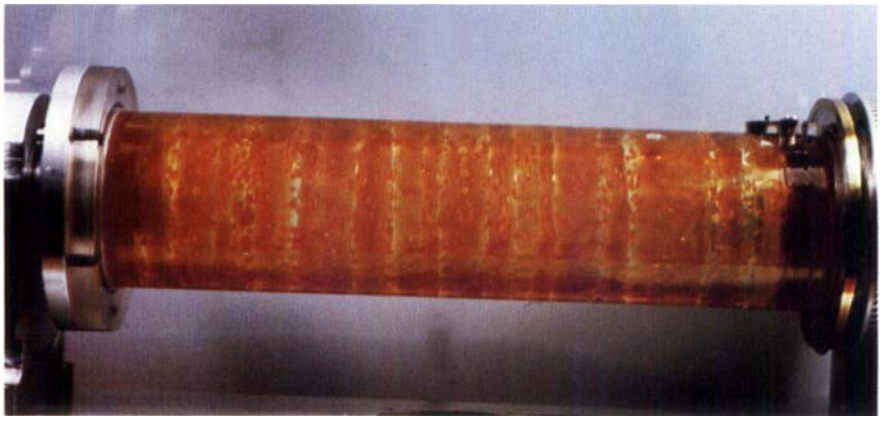

FIGURE 29. Monograde motor oil (brown) and water (clear).

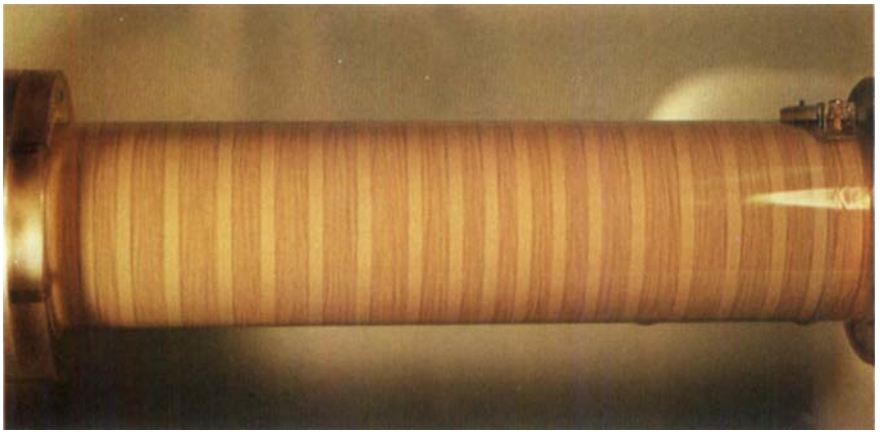

FIGURE 30. Monograde motor oil (SAE40) and water at $\Omega = 440$ r.p.m. The light cells are emulsions of oil with small droplets of water. The dark cells are of water with many large drops of oil.